

Stereocontrol Strategies in Asymmetric Organic Photochemical Synthesis

Xuan Jiang^{1†}, Xu Han^{2†}, Fu-Dong Lu¹, Liang-Qiu Lu^{1*}, Zhiwei Zuo^{2*} & Wen-Jing Xiao^{1,2,3*}

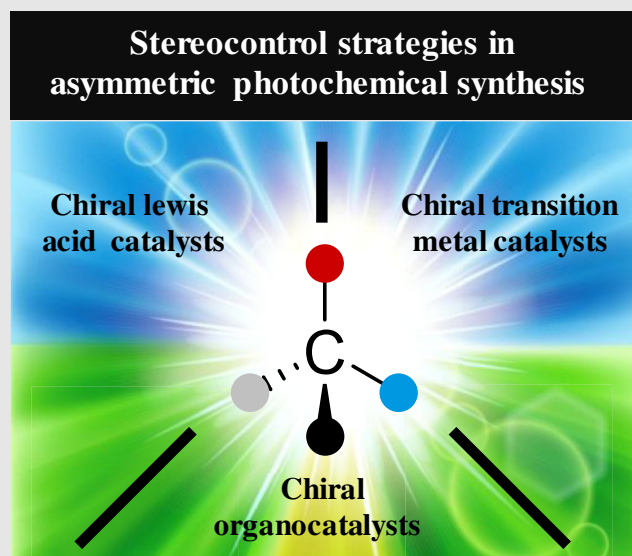
¹Engineering Research Center of Photoenergy Utilization for Pollution Control and Carbon Reduction, Ministry of Education, College of Chemistry, Central China Normal University, Wuhan 430079, ²State Key Laboratory of Organometallic Chemistry, Shanghai Institute of Organic Chemistry, Chinese Academy of Sciences, Shanghai 200032, ³Wuhan Institute of Photochemistry and Technology, Wuhan 430082

*Corresponding authors: luliangqiu@mail.ccnu.edu.cn; zuozhw@shanghaitech.edu.cn; wxiao@mail.ccnu.edu.cn;
†X. Jiang and X. Han contributed equally to this work.

Cite this: *CCS Chem.* **2025**, 7, 1567–1602

DOI: 10.31635/ccschem.025.202505512

Visible light-induced asymmetric organic photochemical synthesis has received growing attention since the first pioneering report into the enantioselective α -alkylation of aldehydes via dual photoredox and amine catalysis. The evolution of this area over the past few decades has provided the synthetic community with a unique tool for obtaining previously challenging, and even unavailable, chiral molecules via an attractive protocol. This review briefly introduces the general stereocontrol strategies for asymmetric photochemical transformations under the classification of organocatalysis, Lewis acid catalysis, and transition metal catalysis. Moreover, opportunities and challenges in this emerging area are noted from this perspective.

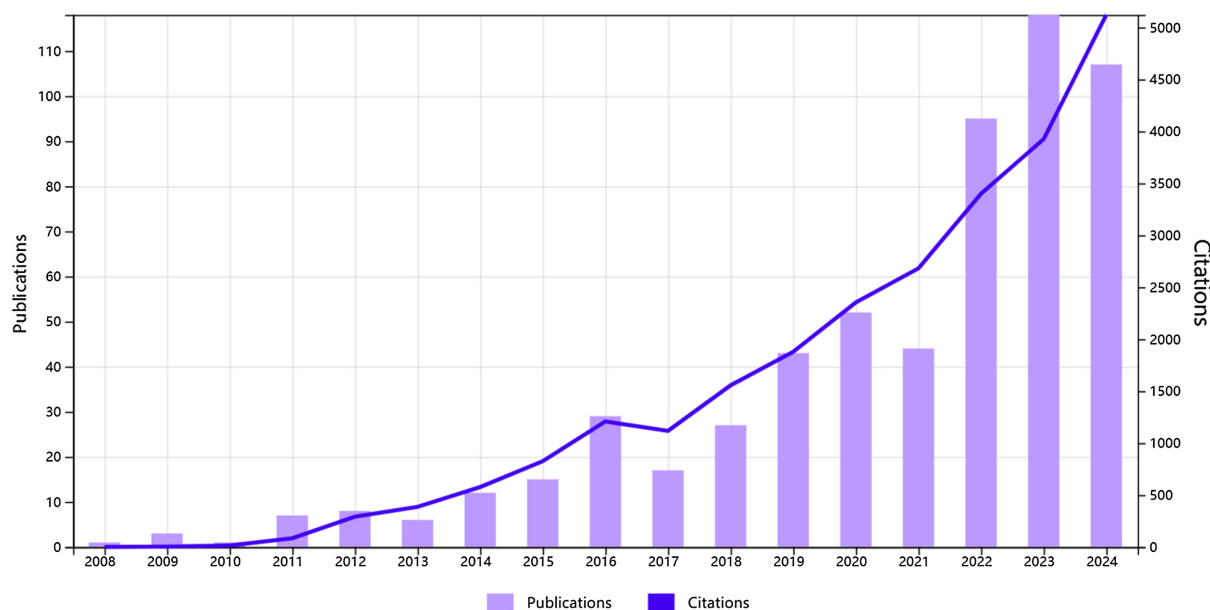


Keywords: photochemical synthesis, asymmetric catalysis, dual catalysis, bifunctional catalysis, stereocontrol strategies

Introduction

Chiral molecules can possess unique physical and chemical properties that render them of fundamental significance in the fields of medicine, biology, and material science.¹ Among the most efficient approaches reported for the preparation of these substances, asymmetric

catalysis stands out as a green, economic, and powerful strategy, with the 2001 Nobel Prize in Chemistry being awarded to Knowles, Sharpless, and Noyori for their work in this area.² Twenty years later, the Nobel Prize in Chemistry was awarded to List and MacMillan for their research in asymmetric catalysis,³ further attesting to the immense potential of this strategy. In addition, over the past few



Scheme 1 | *Asymmetric catalysis publications and citations over time, up to 2024.*

decades, the asymmetric catalysis of thermal reactions has developed rapidly, transitioning into a mature and systematic discipline.^{4,5} Nevertheless, from the perspective of green and sustainable synthetic chemistry, the development of new catalytic strategies for breaking inert chemical bonds and converting easily available feedstocks to value-added final chemicals remains highly desirable.

As a sustainable energy source, light has proven to be powerful in reducing the activation energies of chemical transformations.^{6–9} Unlike traditional thermal reactions, photochemistry can produce radicals and other reactive intermediates under mild conditions, offering an opportunity for new strategies in asymmetric catalysis and chemical synthesis (Scheme 1). As early as 2005, Bach and coworkers¹⁰ developed a chiral bifunctional catalyst by combining a photosensitizer unit and a hydrogen-bonding unit to generate a bifunctional catalyst and realize the first asymmetric intramolecular C–H addition reaction under ultraviolet light irradiation. In 2008, Nicewicz and MacMillan¹¹ developed a dual catalysis system by combining a chiral organic amine catalyst and a Ru-based photosensitizer, which promoted the first intermolecular asymmetric alkylation of aldehydes under visible light irradiation. These great successes are attributed to the important fact that photochemical excitation, especially that induced by visible light, shows great potential in the activation of inert chemical bonds and the generation of highly active intermediates under mild conditions, which are beneficial for good compatibility of functional groups, safety of manipulators and economy of production. By strategically combining this approach with general asymmetric chemical catalysis

(including asymmetric organocatalysis, asymmetric Lewis acid catalysis, and asymmetric transition metal catalysis), a variety of visible light-induced, enantioselective organic photochemical reactions have been successfully developed in recent decades.^{12–19}

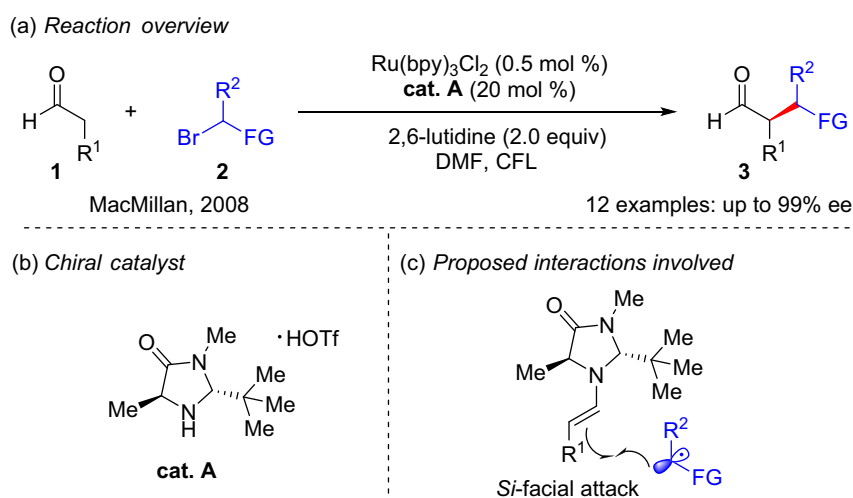
In contrast to previous reviews in this field that have focused on reaction conversions and principles, the current review systematically presents the stereocontrol strategies of asymmetric photochemical transformations and highlights the challenges existing in this emerging field, aiming to provide a brief reference for future research. Although enantioselective organic photoreactions enabled by asymmetric enzyme catalysis constitute another efficient strategy to supplement asymmetric chemical catalysis, these are considered beyond the scope of this review, but have been addressed in a recent review by Kourist and Kroutil.²⁰

Asymmetric Photocatalysis with Organocatalysis

Visible light induced asymmetric enamine and iminium catalysis

Visible light induced asymmetric enamine catalysis

Enamine catalysis is a classic approach to the activation of carbonyl compounds upon condensation with amine catalysts.²¹ Due to the p– π conjugation effect, the energy of the highest occupied molecular orbital of the enamine intermediate is generally increased, facilitating their reaction with electrophilic radicals. In 2008, Nicewicz and

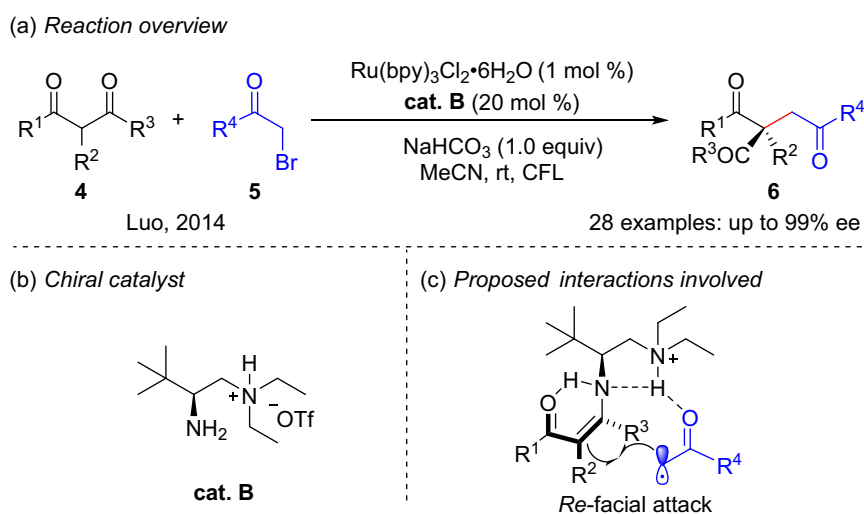


Scheme 2 | Photocatalytic asymmetric α -alkylation of aldehydes using a chiral secondary amine catalyst.

MacMillan¹¹ developed a photoinduced asymmetric α -alkylation of aldehydes bearing electrodeficient halides via the combination of a ruthenium photocatalyst with a chiral secondary amine catalyst (Scheme 2). In this reaction, density functional theory (DFT) calculations have been used to explain the stereochemical output. More specifically, the amine catalyst undergoes a condensation reaction with the aldehyde to selectively form an enamine species, leading to the generation of a p - π conjugated (*E*)-olefin far from the bulky *tert*-butyl group, which minimizes any nonbonding interactions with the imidazolidinone ring. The methyl group on the catalyst effectively shields the *Re*-face of the enamine, leading to radical addition from the *Si*-face. The same group also reported that enamines can be oxidized by an excited-state photocatalyst via a single-electron transfer (SET)

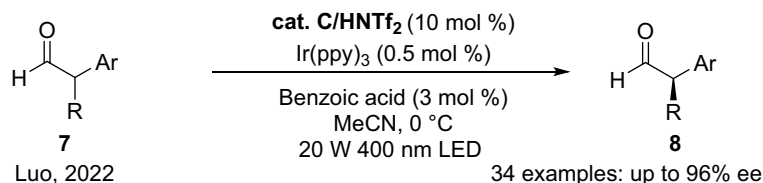
process to form a chiral radical intermediate, which undergoes a subsequent asymmetric radical transformation.²² Similarly, the bulky group on the chiral catalyst greatly affects the stereoselectivity.

Primary amine catalysts have also been demonstrated to efficiently promote asymmetric transformations of ketones, which are more sterically crowded than aldehydes.²³ In 2014, Luo and coworkers²⁴ realized the asymmetric α -alkylation of β -ketocarbonyl compounds to directly construct chiral all-carbon quaternary stereocenters by combining a photocatalyst with a primary amine catalyst (Scheme 3). Based on their previous work,²⁵ these authors proposed that the hydrogen bonding network plays a critical role in this reaction. More specifically, intramolecular hydrogen bonding in the enamine increases the rigidity of the molecular skeleton,

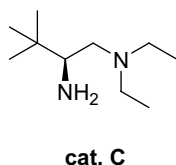


Scheme 3 | Photocatalytic asymmetric α -alkylation of β -ketocarbonyl compounds using a chiral primary amine catalyst.

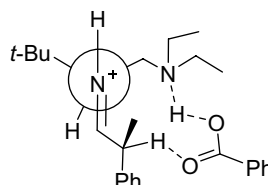
(a) Reaction overview



(b) Chiral catalyst



(c) Proposed interactions involved



Scheme 4 | Photocatalytic deracemization of aldehydes using a chiral primary amine catalyst.

resulting in the *Re*-face being more exposed. In addition, hydrogen bonding interactions between the protonated tertiary amine and the α -carbon radical greatly shorten the distance between the two intermediates, further promoting attack at the *Re*-face. Consequently, all-carbon quaternary stereocenters were generated with good enantioselectivities.

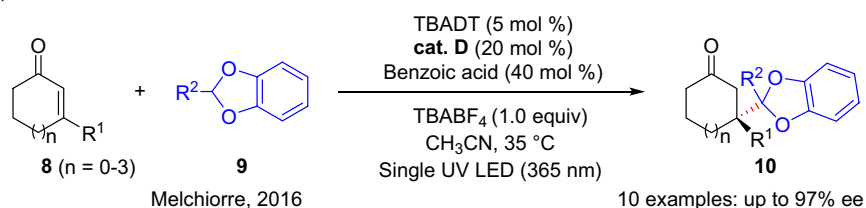
Aryl-substituted enamine intermediates can undergo an energy transfer process with an excited-state photocatalyst to achieve *E/Z* isomerization owing to the difference in the excited triplet energies of the *E/Z* configurations. Employing this strategy, Luo and coworkers²⁶ integrated amine catalysis with visible-light catalysis, achieving the highly selective racemization of α -branched aldehydes (Scheme 4). In the ground state,

the stereochemically matched enantiomer preferentially formed the *E*-enamine, which continuously isomerized to the *Z*-enamine via photocatalytic energy transfer. Subsequently, the *Z*-enamine underwent proton-transfer shuttle conversion to the mismatched enantiomer. Notably, the stereospecificity of the chiral primary amine-catalyzed enamine protonation is crucial for ensuring a high product enantioselectivity.

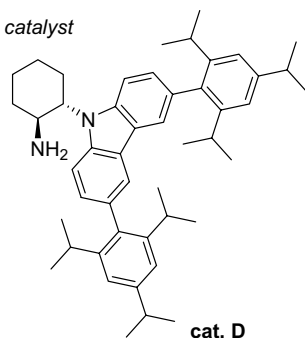
Visible light induced asymmetric iminium catalysis

Iminium catalysis refers to the conjugated addition or cycloaddition reaction of α,β -unsaturated carbonyl compounds and nucleophiles under the action of an amine

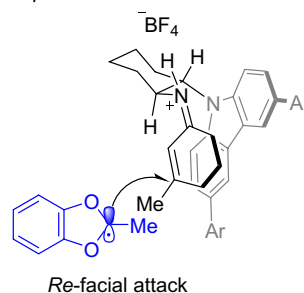
(a) Reaction overview



(b) Chiral catalyst



(c) Proposed interactions involved



Scheme 5 | Photocatalytic asymmetric radical conjugated addition using a chiral primary amine catalyst.

catalyst.²⁷ In this reaction, the key process involves the condensation of amine catalysts and carbonyl compounds to form imine intermediates, which possess a lower lowest unoccupied molecular orbital energy, thereby rendering nucleophilic attack more facile. In 2016, Melchiorre and coworkers²⁸ reported an asymmetric radical conjugate addition to α,β -disubstituted cyclic enones via photocatalytic C–H activation. As shown in Scheme 5, imine ions exist in a single *Z*-configuration due to intramolecular charge transfer between the electron-rich carbazole and the electron-deficient iminium ion. More specifically, this involved π - π interactions, as confirmed by X-ray single-crystal analysis. These interactions also result in the carbazole moiety shielding the imine *Si*-face, leaving the *Re*-face exposed for enantioselective radical addition reactions.

Visible light induced asymmetric nucleophilic catalysis

Visible light induced asymmetric *N*-heterocyclic carbene catalysis

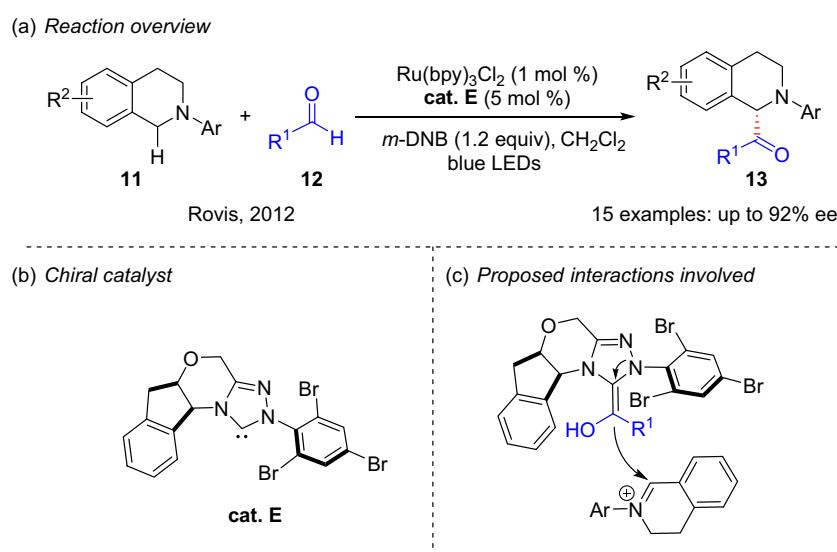
N-Heterocyclic carbene (NHC) catalysis is a powerful strategy to reverse the polarity of aldehydes and their derivatives, which makes them efficient nucleophiles.²⁹ In 2012, DiRocco and Rovis³⁰ described an enantioselective α -C–H acylation of tertiary amines with aldehydes by merging asymmetric NHC catalysis and visible light photocatalysis (Scheme 6). In that work, the authors skillfully used single electron photooxidation to generate active imine ions, which were captured by chiral Breslow intermediates formed by aldehydes and NHC catalysts. The specific stereocontrol model was not illustrated, so an approximate model was proposed based on previous work on the polarity-reversed transformations of

aldehydes with imines.²⁹ Notably, the indenyl group on the Breslow intermediate blocks one side of the enol to ensure the face selectivity of the reaction, while the *N*-aryl group of the NHC catalyst imparts a certain steric hindrance on the imine ion, promoting attack of the enol from a single direction.

The Breslow intermediates formed during the above process can subsequently generate chiral radicals via SET, thereby achieving the β -functionalization of α,β -unsaturated aldehydes. In 2022, Hong and coworkers³¹ achieved the photoinduced asymmetric β -pyridylation of enals using chiral NHC catalysts (Scheme 7). As a substrate, the pyridinium salts formed electron donor-acceptor complexes with the Breslow intermediate-derived homoenolates to induce radical generation, in addition to effectively controlling the pyridyl C4-selectivity of the radical addition protocol. Furthermore, the use of hexafluorobenzene as a solvent significantly strengthened the interaction between the chiral homoenolate and the pyridinium salt, thereby enhancing the stereoselectivity.

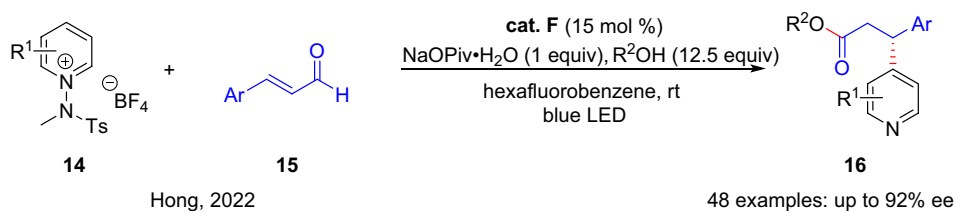
Visible light induced asymmetric tertiary amine catalysis

The iminium ions produced by photooxidation have also been used in other nucleophilic catalytic reactions. For example, in 2014, Xiao and coworkers³² implemented the direct sp^3 C–H acroleination of *N*-aryl-tetrahydroisoquinoline (THIQ) via sequential photoredox and tertiary amine catalysis. One asymmetric example was described using β -isocupreidine (β -ICD) as the chiral nucleophilic catalyst, achieving moderate enantioselectivity. Two years later, Jiang and coworkers³³ disclosed that the addition of NaBARF could significantly improve the

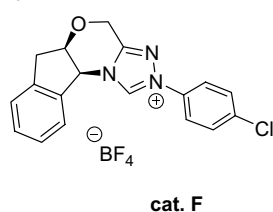


Scheme 6 | Photocatalytic asymmetric α -C–H acylation of tertiary amines using a chiral NHC catalyst.

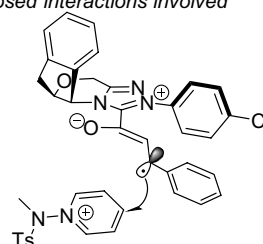
(a) Reaction overview



(b) Chiral catalyst



(c) Proposed interactions involved



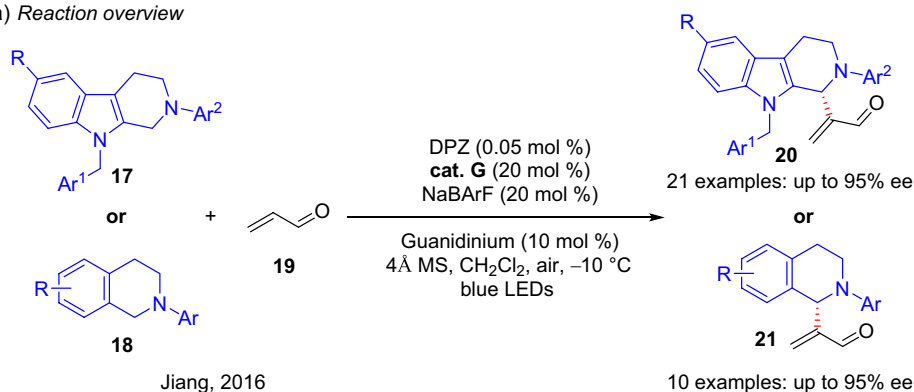
Scheme 7 | Photoinduction asymmetric β -pyridylation of enals using a chiral NHC catalyst.

enantioselectivity of this reaction (Scheme 8). The authors suggested that NaBARF plays multiple roles, activating acrolein as a Lewis acid to promote the formation of nucleophilic intermediates, acting as a counterion to stabilize the iminium ions, and providing a chain to bridge the nucleophilic intermediates and iminiums via multisite coordination. Ultimately, these effects resulted in an enhanced chemoselectivity and amplified chiral induction by β -ICD.

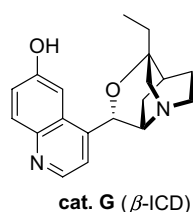
Visible light induced asymmetric hydrogen-bonding catalysis

In addition to asymmetric valent-bonding catalysis, non-valent bonding stereocontrol strategies have also been widely used in asymmetric organocatalysis.³⁴ In particular, asymmetric hydrogen-bonding catalysis has recently been successfully applied in various enantioselective organic photochemical transformations, which are complementary to the above reaction types and substrate scope

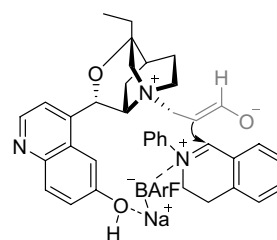
(a) Reaction overview



(b) Chiral catalyst

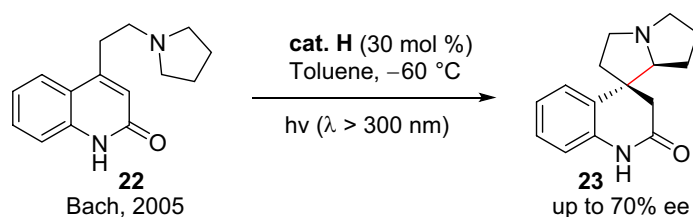


(c) Proposed interactions involved

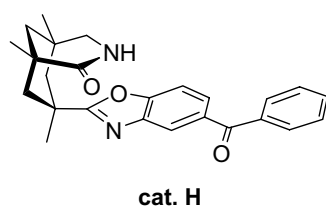


Scheme 8 | Photocatalytic asymmetric C-H acroleination of THIQ using a chiral tertiary amine catalyst.

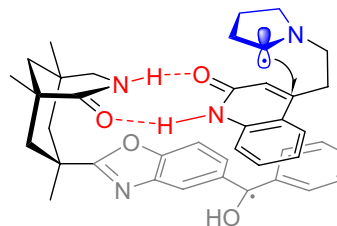
(a) Reaction overview



(b) Chiral catalyst



(c) Proposed interactions involved



Scheme 9 | Photocatalytic asymmetric intramolecular radical addition using a chiral bifunctional catalyst.

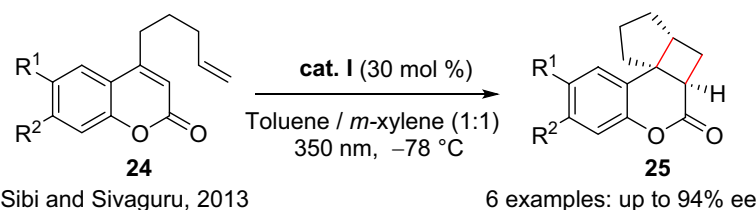
examples. In this section, the recent advances in this field are highlighted in terms of the hydrogen-bonding donors.

Visible light induced asymmetric amide catalysis

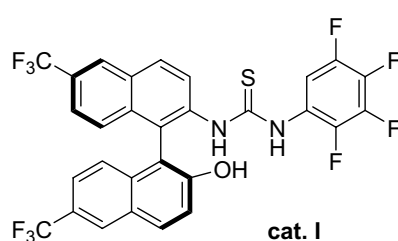
In 2005, Bach and coworkers¹⁰ pioneered the photocatalytic asymmetric intramolecular radical addition reaction through the development of bifunctional hydrogen-bonding photocatalysts. As outlined in Scheme 9, the formation of double hydrogen bonds between the

substrate and the two amide units in the chiral photocatalyst shortens the distance between the pyrrolidine group and the photosensitive unit, thereby facilitating the hydrogen atom transfer (HAT) process. At the same time, the vertical direction of the ordered proximity causes the benzophenone group to shield the bottom of the substrate; thus, radical attack on the olefin is favored from the top of the complex. Later, Bach further optimized a bifunctional photocatalyst by replacing benzophenone with thioxanthone to achieve the visible light-induced enantioselective [2+2] cycloaddition and deracemization of chiral allenes.^{35,36}

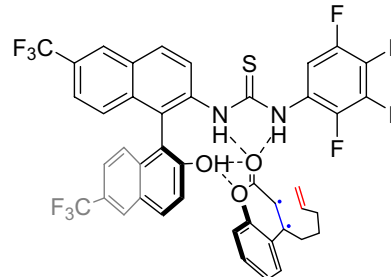
(a) Reaction overview



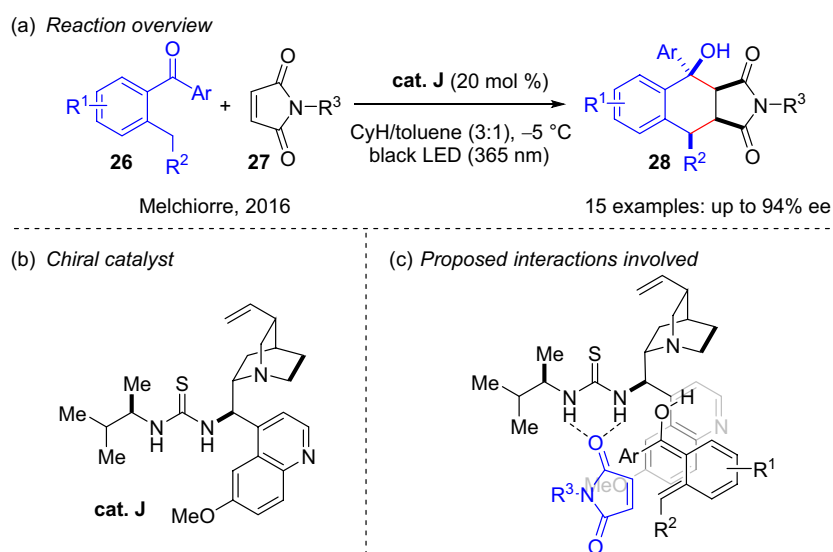
(b) Chiral catalyst



(c) Proposed interactions involved



Scheme 10 | Photocatalytic asymmetric [2+2] cycloaddition using a chiral thiourea catalyst.



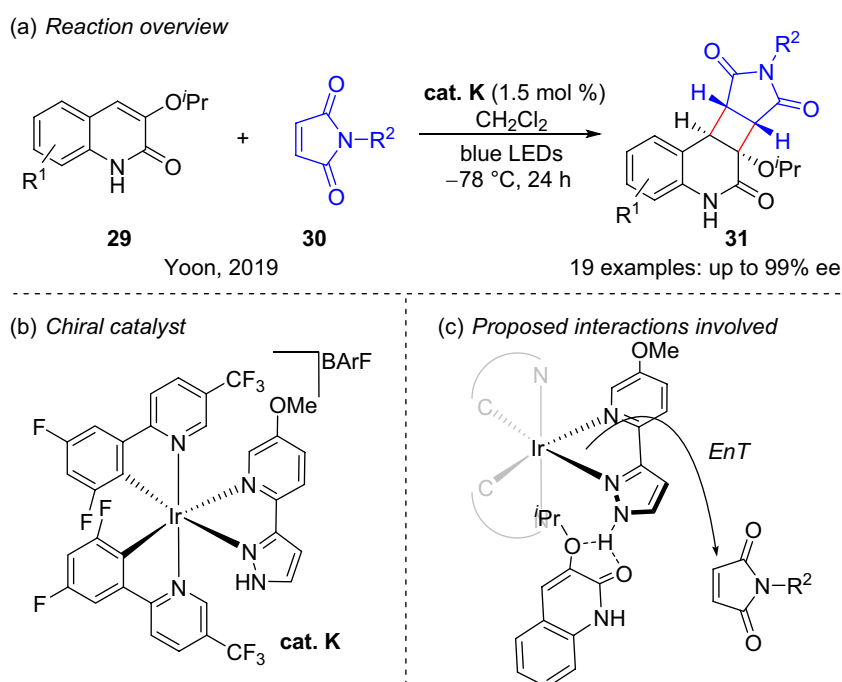
Scheme 11 | Photoinduced asymmetric Diels–Alder reaction using a chiral thiourea catalyst.

Visible light induced asymmetric thiourea catalysis

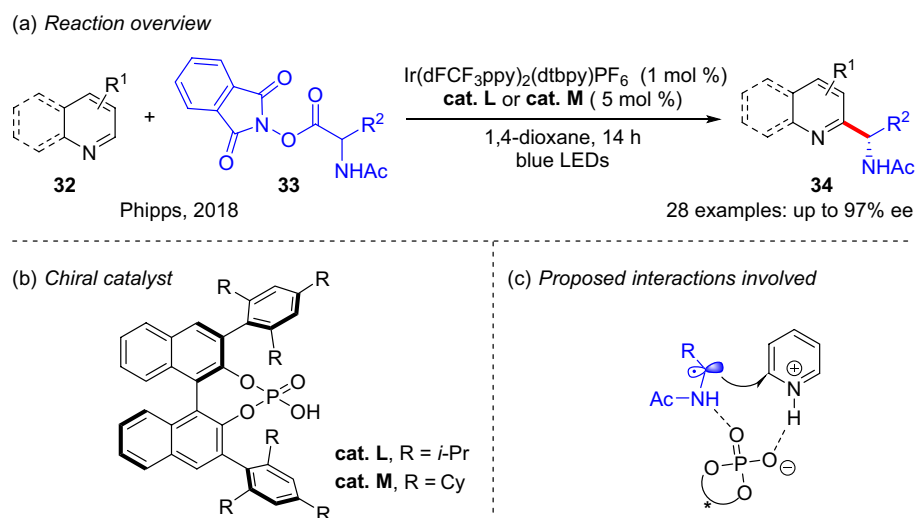
In 2013, Sivaguru and coworkers³⁷ reported the asymmetric [2+2] photocycloaddition of 4-alkenyl-substituted coumarins using a chiral thiourea catalyst, producing structurally complex chiral coumarins in good enantioselectivities (Scheme 10). A series of control experiments and photophysics studies were performed, and the authors proposed that a hydrogen bonding network

model between the catalyst and substrate helped reduce the triplet energy of the coumarin. In addition, the rigid structure caused the olefins in the side chain to deviate from the complex, resulting in a good enantioselectivity.

In 2016, Melchiorre and coworkers³⁸ realized an asymmetric Diels–Alder reaction between maleimides and photochemically generated hydroxy-*o*-quinodimethanes using asymmetric thiourea catalysis (Scheme 11). In this system, the key factor in suppressing the racemic



Scheme 12 | Photocatalytic asymmetric intermolecular [2+2] cycloaddition by a chiral pyrazole catalyst.



Scheme 13 | Photocatalytic asymmetric Minisci-type addition using a chiral phosphoric acid catalyst.

background reaction was the content of the photo-generated hydroxyl-*o*-quinodimethane, which could be controlled by reversible electron transfer between the quinuclidine moiety and the excited benzophenone. Furthermore, the thiourea moiety acted as a chiral catalyst, increasing the electrophilicity of the maleimide via double hydrogen bonding activation, whilst also inducing the enantioselectivity of the Diels–Alder process.

Visible light induced asymmetric pyrazole catalysis

Compared with intramolecular processes,³⁹ asymmetric intermolecular [2+2] cycloadditions are more challenging due to the instability of the biradical species.⁴⁰ A breakthrough in this area was achieved by Yoon and coworkers⁴¹ in 2019, who realized an asymmetric [2+2] cycloaddition of 3-alkoxyquinolones and maleimides through the use of a chiral hydrogen bonding iridium photosensitizer (Scheme 12). DFT calculations showed that the energy of the hydrogen bonding complex reaches its lowest level when the pyrazole forms double hydrogen bonds with the two oxygen atoms of the 3-alkoxyquinolone, and when the *Re*-face of the 3-alkoxyquinolone is close to the Ir complex. Subsequently, the triplet-state maleimide can attack the quinolone from the *Si*-face only.

Visible light induced asymmetric phosphoric acid catalysis

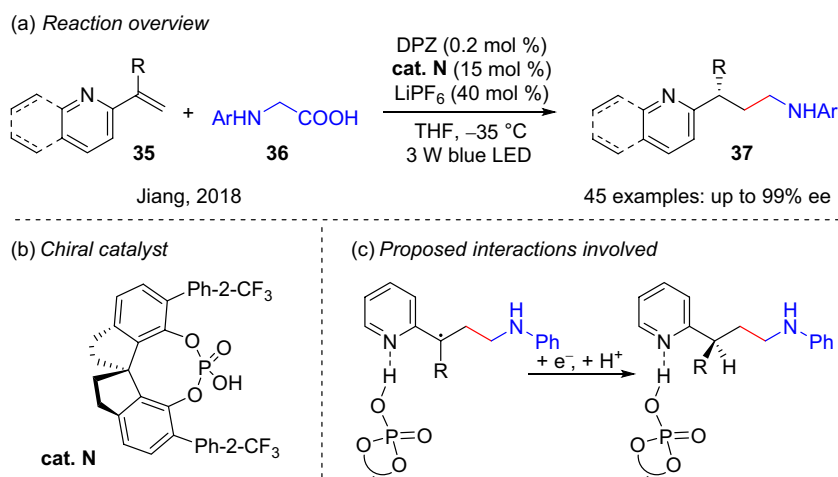
In 2018, Phipps and coworkers⁴² reported a visible light-induced enantioselective Minisci-type addition to heteroarenes using an amino acid-derived redox active ester and asymmetric phosphoric acid catalysis (Scheme 13). Through control experiments, they found that the NH bond on the radical precursor is key to achieving a high

enantioselectivity. In the absence of this bond, the reaction proceeded well, but no stereoselectivity was observed. Therefore, chiral phosphoric acid can be used as a Brønsted acid catalyst to activate heteroarenes, in addition to forming hydrogen bonds with radicals to accelerate the Minisci-type addition. Moreover, the large steric hindrance imparted by the 3,3'-substituents of the binaphthyl subunits provides a suitable chiral cavity to control the stereoselectivity.

Similarly, Jiang and coworkers⁴³ reported the enantioselective radical conjugate addition reaction of α -aryl glycines to α -branched 2-vinylpyridines and 2-vinylquinolines via dual visible light photoredox and chiral phosphoric acid catalysis (Scheme 14). In contrast to the work of Phipps et al.,⁴² the stereoselectivity of this reaction was controlled by enantioselective protonation, as supported by DFT calculations. The authors proposed that the aryl group of the catalyst provides a suitable steric effect, leading to the enantioselective protonation of the favored face.

Asymmetric protonation via proton shuttling is another common catalytic mechanism for chiral phosphoric acid formation. In 2022, Jiang and coworkers⁴⁴ reported the photocatalytic racemization of α -amino esters and ketones using chiral phosphoric acid catalysts (Scheme 15). In this reaction, the photocatalysis process transformed the racemic α -amino esters into prochiral enol intermediates, which subsequently underwent asymmetric protonation through the proton shuttle mechanism to generate a single configuration of α -amino esters. DFT calculations showed that the presence of multiple hydrogen bonds in the enol and chiral phosphoric acid catalysts was critical for achieving enantiomeric enrichment.

In 2021, Bach and coworkers⁴⁵ combined photosensitive thioxanones with a chiral phosphoric acid scaffold



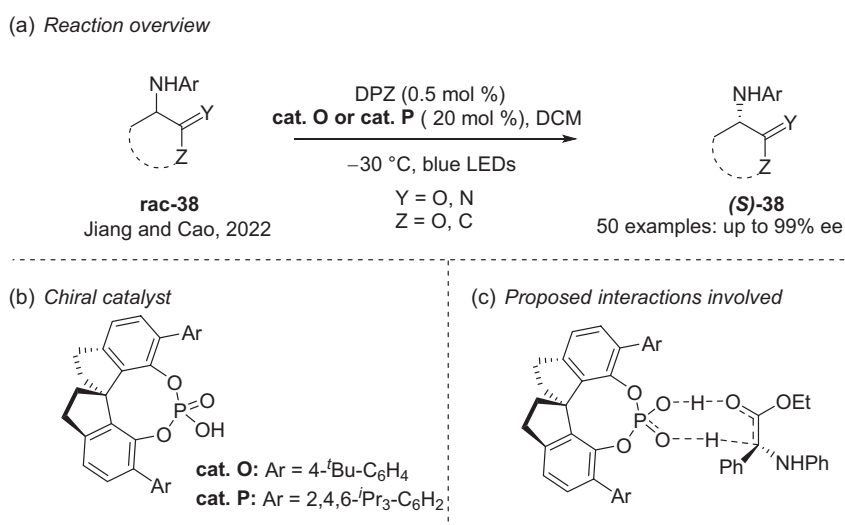
Scheme 14 | Photocatalytic asymmetric radical conjugate addition using a chiral phosphoric acid catalyst.

to achieve a photoinduced asymmetric [2+2] cyclization reaction (Scheme 16). The imine ion intermediate formed from the acetal imine under acidic conditions enhanced olefin conjugation, thereby lowering the triplet energy. Moreover, the imine ion formed multiple hydrogen bonds with the phosphate anions, which not only brought the photosensitive fragment closer to the olefin, but it also created a chiral reaction environment, allowing the olefin of another molecule to attack exclusively from the *Si* face.

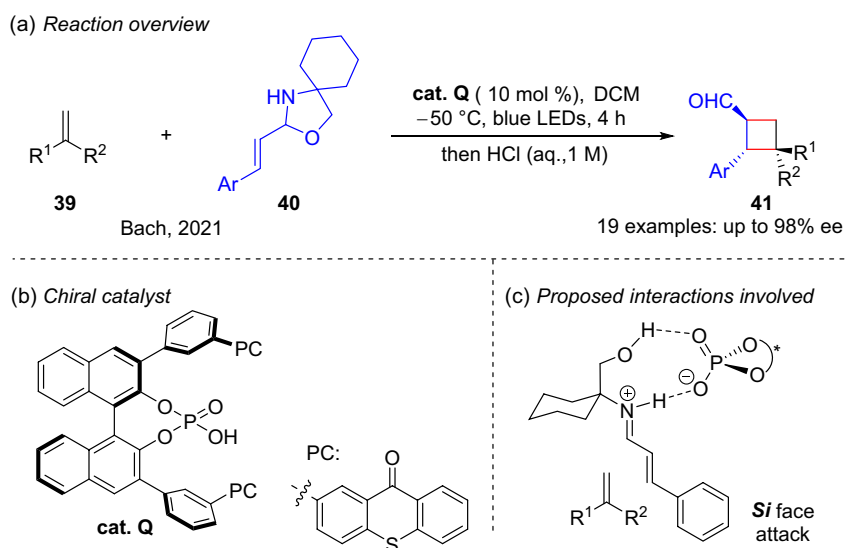
Visible light induced asymmetric Brønsted base and HAT catalysis

In 2019, Knowles and coworkers⁴⁶ developed a deracemization reaction of cyclic urea compounds via a sequence of electron, proton, and HAT processes. As

shown in Scheme 17, the enantioselectivity of this conversion was well controlled via two chiral catalysts, a phosphate base, and a peptide-based thiol. In this process, the (*S*)-configuration phosphate base, which is stereo-matched with the (*S*)-configuration urea radical cation (generated via single electron photooxidation), renders the intermediate more prone to deprotonation, generating a racemic α -amino radical. The stereo-unmatched (*R*)-intermediate is then reverted back to the starting material by the reduced-state photocatalyst, resulting in an enrichment of the slow-reacting (*R*)-cyclic urea. Moreover, when the chiral thiols acts as a hydrogen donor, the (*R*)-enantiomer is favorably produced owing to the enantioselective HAT process of the racemic α -amino radical, thereby further increasing the enantiopurity of the (*R*)-enantiomer. Control experiments showed that regardless of the chiral catalyst used, the



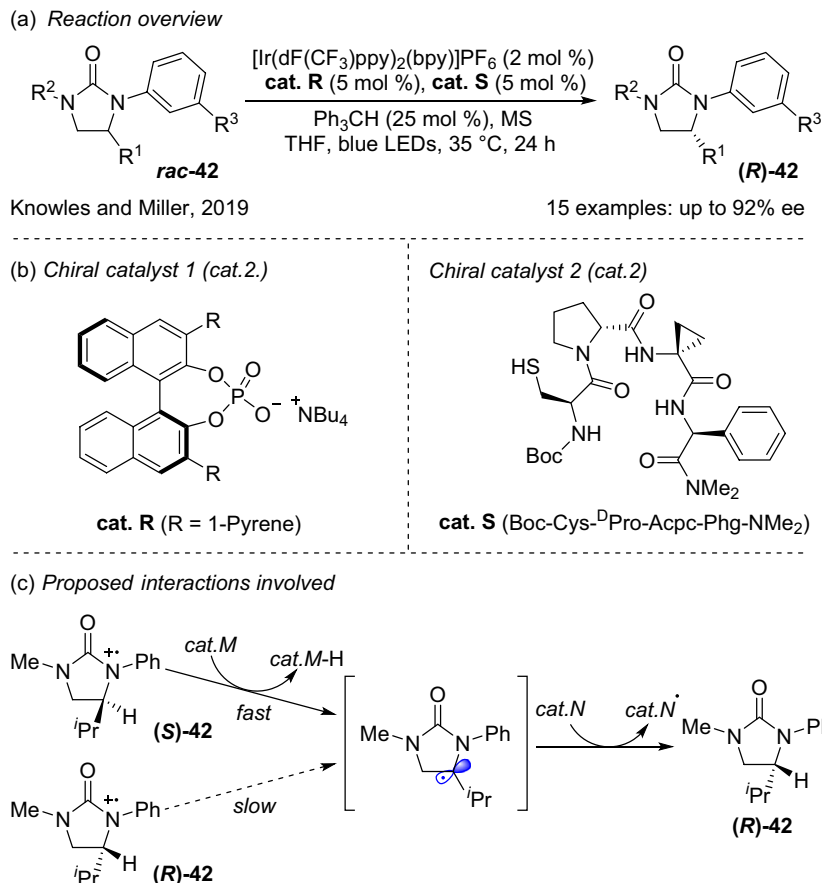
Scheme 15 | Photocatalytic deracemization of α -amino esters using a chiral Brønsted acid catalyst.



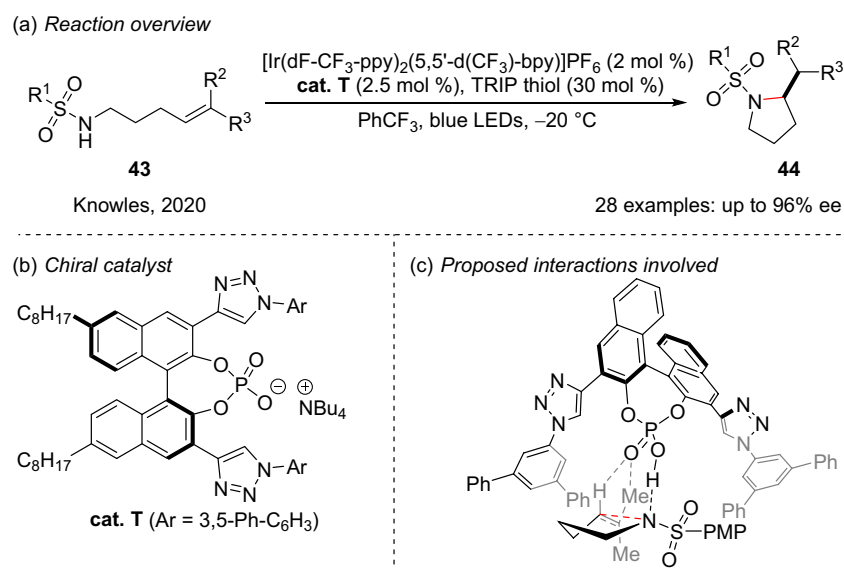
Scheme 16 | Asymmetric [2+2] photocycloaddition using a sensitizing chiral phosphoric acid catalyst.

reaction did not achieve a good stereoselectivity. These results indicate that synergy is required between the two chiral catalysts in this transformation to achieve high enantioselectivity.

In this multicatalytic system, even a single chiral catalyst was able to achieve excellent stereoselective control. More specifically, in 2020, Knowles and coworkers⁴⁷ reported the photocatalytic intramolecular asymmetric



Scheme 17 | Photocatalytic deracemization using a chiral Brønsted base catalyst and HAT catalyst.

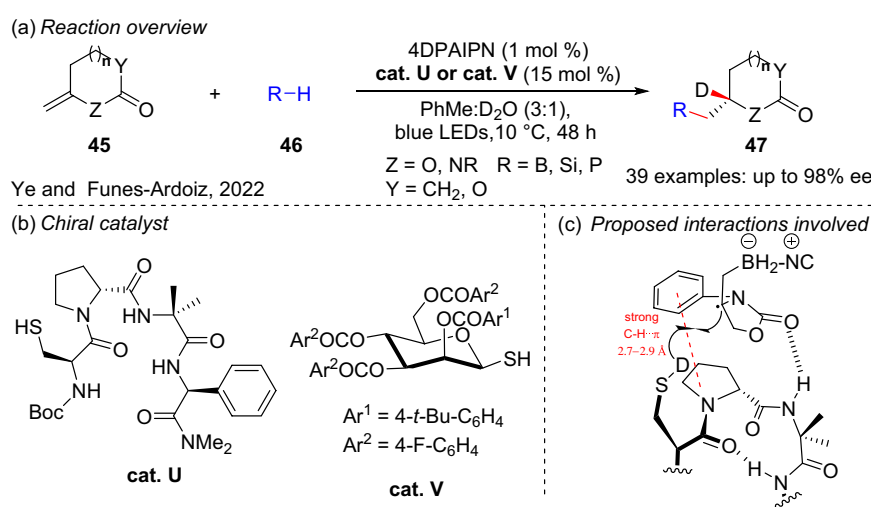


Scheme 18 | Photocatalytic asymmetric hydroamination of alkenes using a chiral Brønsted base catalyst.

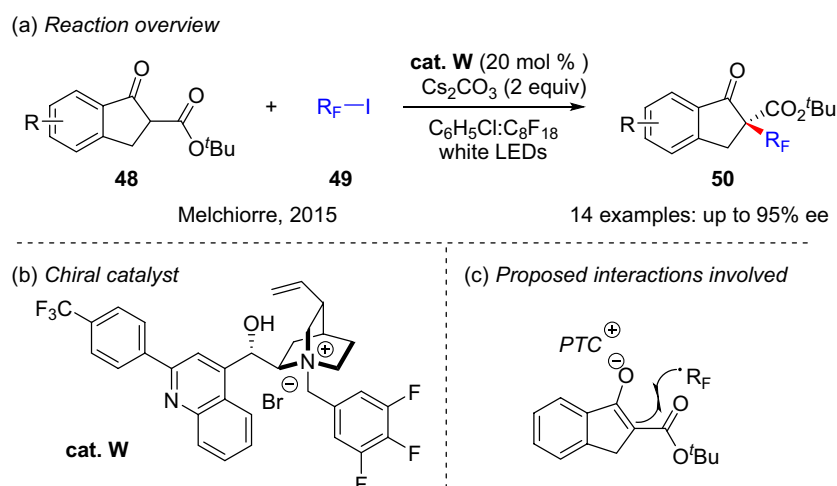
hydroamination of olefins using chiral phosphates (Scheme 18). In this process, the sulfonamides generate *N*-centered radicals through proton-coupled electron transfer in the presence of chiral phosphate anions, and the resulting sulfonamidyl radicals retain strong multiple hydrogen bonding interactions with chiral phosphate anions. This induces enantioselectivity in the intramolecular radical addition reaction via a cyclic transition state. DFT calculations further revealed the presence of C–H– π interactions between the substrate and the aryl group on the chiral phosphate side chain, significantly enhancing the stereoselectivity.⁴⁸

In 2022, Ye and coworkers⁴⁹ realized a photocatalytic asymmetric radical deuteration protocol using chiral

thiols as the HAT catalysts and D₂O as the deuterium source (Scheme 19). This reaction proceeded through the addition of heteroatom radicals to exocyclic olefins, followed by a subsequent stereospecific HAT process involving the deuterated chiral thiols. Consequently, products exhibiting a high deuteration rate were obtained. DFT calculations revealed that hydrogen bonding between the carbonyl group of the substrate and the amide of the catalyst shaped the spatial configuration of the transition state. Moreover, C–H– π interactions between the proline and the phenyl ring of the radical adduct restricted the HAT process, ensuring that it occurred exclusively on the *Si* face.



Scheme 19 | Photocatalytic asymmetric radical deuteration using an HAT catalyst.



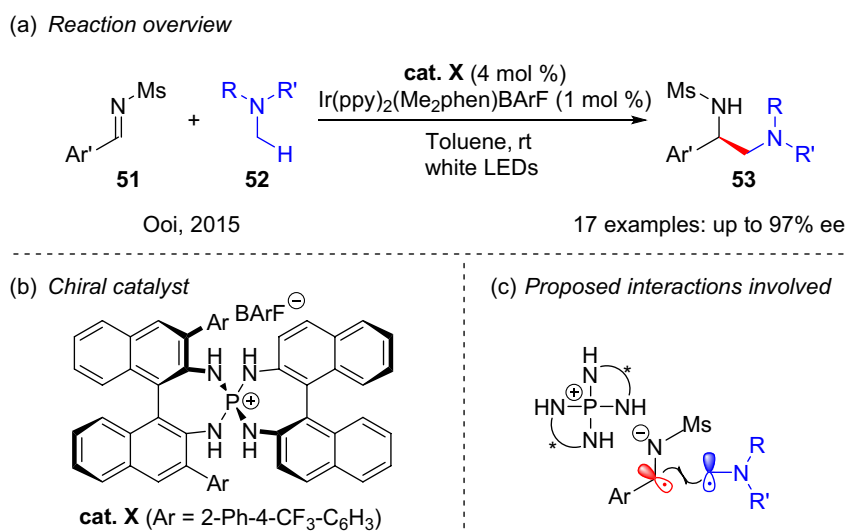
Scheme 20 | Photoinduced asymmetric perfluoroalkylation of β -ketoesters using a chiral N-centered PTC.

Visible light induced asymmetric phase transfer catalysis

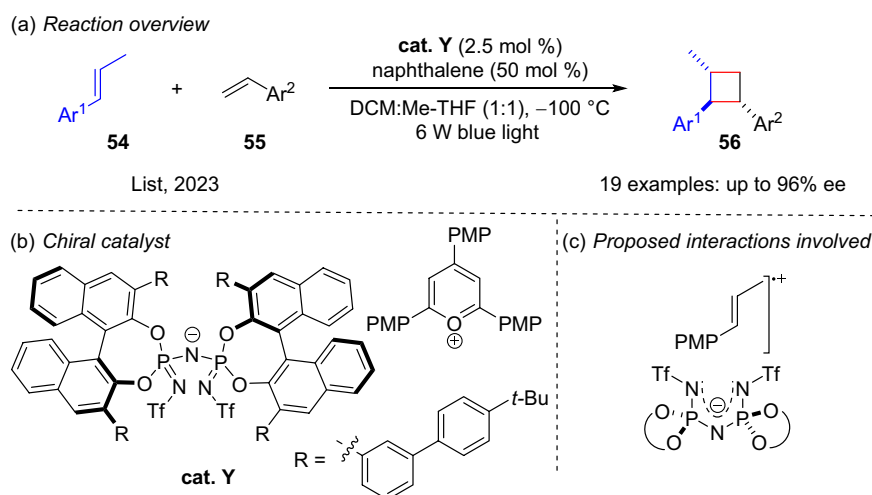
Asymmetric phase transfer catalysis is one of the most effective methods to achieve the stereoselective transformation of ionic intermediates.⁵⁰ For example, in 2015, Melchiorre and coworkers⁵¹ realized enantioselective perfluoroalkylation of cyclic β -ketoesters using a chiral quaternary ammonium salt catalyst under white light irradiation (Scheme 20). In this system, three potential interactions were proposed between the substrate and the chiral phase transfer catalyst (PTC), namely electrostatic interactions between the quaternary ammonium salt and the enolate, hydrogen bonding interactions between the hydroxyl group of the PTC and the ester group of the substrate, and finally, π - π interactions between the

PTC benzyl group and the aromatic portion of substrate. Therefore, radical attack on the *Si*-face of the enolate-PTC complex was favored.

Also in 2015, Ooi and coworkers⁵² reported the asymmetric radical coupling of *N*-arylaminoethanes with aldimines through the combined use of a chiral PTC and a photocatalyst (Scheme 21). Following a series of comparative experiments, the key to achieving a high enantioselectivity was determined to be the use of a *P*-spiro chiral arylaminophosphonium catalyst containing a hydrogen bond donor. This catalyst then combines with the imine radical anion (generated by photoreduction) through electrostatic and hydrogen bonding interactions. Furthermore, the introduction of large steric hindrance groups into the 3,3'-positions of the binaphthyl



Scheme 21 | Photocatalytic asymmetric radical coupling of *N*-arylaminoethanes with aldimines using a chiral *P*-centered PTC.



Scheme 22 | Asymmetric [2+2] cycloaddition via a counteranion-directed photoredox catalyst.

subunits contributes to the creation of a cavity over the ionic hydrogen bonding site, resulting in a significant increase in enantioselectivity.

Chiral anionic catalysts can also be used to control the stereoselectivities of cationic radicals. For example, in 2023, List innovatively employed a combination of sterically hindered imidodiphosphorimidate anions and photosensitive oxonium ions as chiral photocatalysts, achieving high enantioselectivities in the photocatalytic [2+2] cycloaddition reaction between anethole and styrenes (Scheme 22).⁵³ This asymmetric counteranion-directed catalysis strategy exhibited a good generality, allowing modification of the redox properties of the catalyst by adjusting the type of cation without compromising control of the stereoselectivity. Coincidentally, Liao and coworkers⁵⁴ employed the same strategy to develop a highly stereoselective light-induced cationic polymerization process. With a catalyst loading of 50 ppm, both temporal control and stereoselective regulation of the vinyl ether polymerization process were achieved simultaneously, with an isotactic selectivity of 91% *m*.

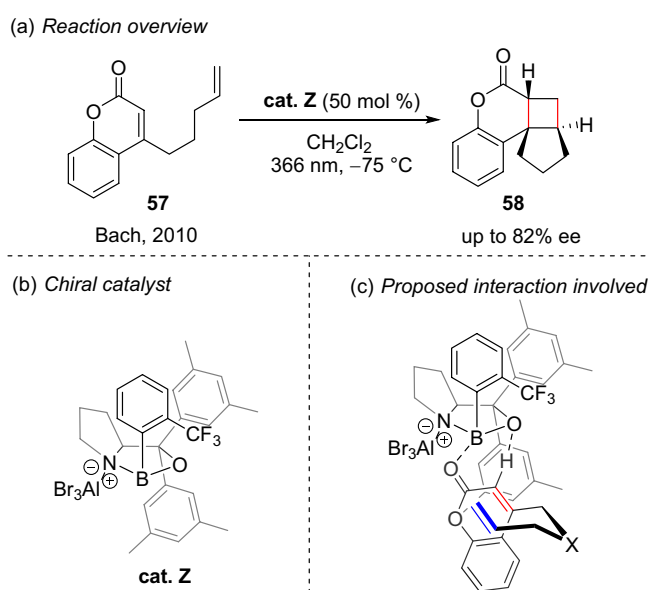
Asymmetric Photocatalysis with Lewis Acid Catalysis

Light absorption shift

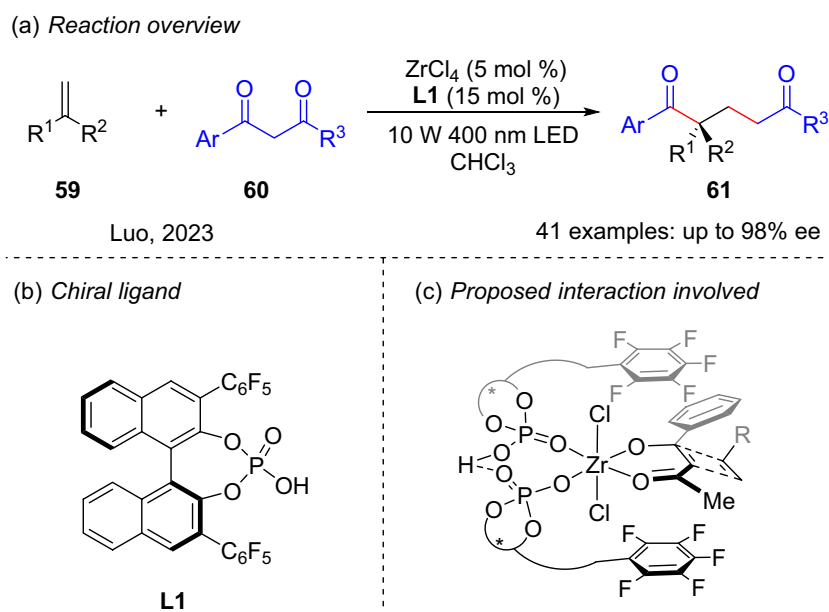
The bathochromic absorption shift caused by the coordination between chiral Lewis acids and certain substrates offers unique opportunities for asymmetric [2+2] photocycloaddition reactions (PCAs).⁴⁰ In 2010, Bach and coworkers reported pioneering work in the area of Lewis acid-catalyzed asymmetric [2+2] PCA reactions (Scheme 23),⁵⁵ in which a chiral oxazaborolidine stood out as an optimal chiral Lewis acid catalyst. As shown in the bottom-right illustration of Scheme 23, the

B–O interaction and the O–H hydrogen bond between the chiral Lewis acid catalyst and the substrate generate a relatively rigid intermediate. Consequently, the terminal alkene attacks the front face of the photoactivated alkene to avoid the steric repulsion imparted by the oxazaborolidine catalyst.

The de Mayo reaction involves an initial [2+2] photocyclization between a 1,3-dicarbonyl compound and an olefin under ultraviolet light, followed by C–C bond cleavage to achieve the bifunctionalization of olefins. In 2023, Luo and coworkers⁵⁶ successfully realized the first visible light-induced asymmetric de Mayo reaction using a chiral zirconium phosphate as a Lewis acid catalyst



Scheme 23 | Photoinduced asymmetric intramolecular [2+2] PCA using a chiral Lewis acid.



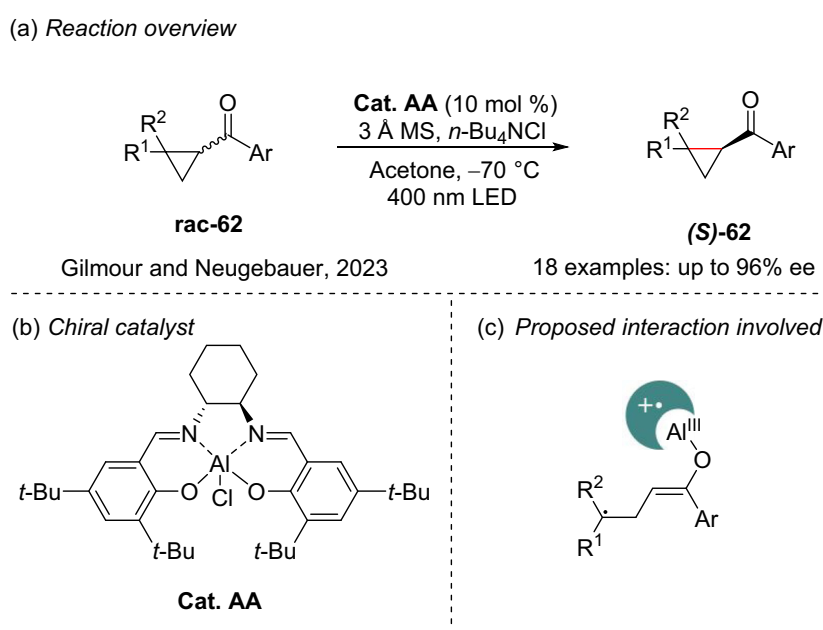
Scheme 24 | Photoinduced asymmetric de Mayo reaction using a chiral zirconium catalyst.

(Scheme 24). This chiral zirconium catalyst not only facilitated formation of the enol intermediate, but it also significantly enhanced its absorbance, thereby effectively preventing background reactions. Additionally, product data analysis suggested that the π - π interaction between the aryl ketone and the olefin influences the stereoselectivity of the reaction.

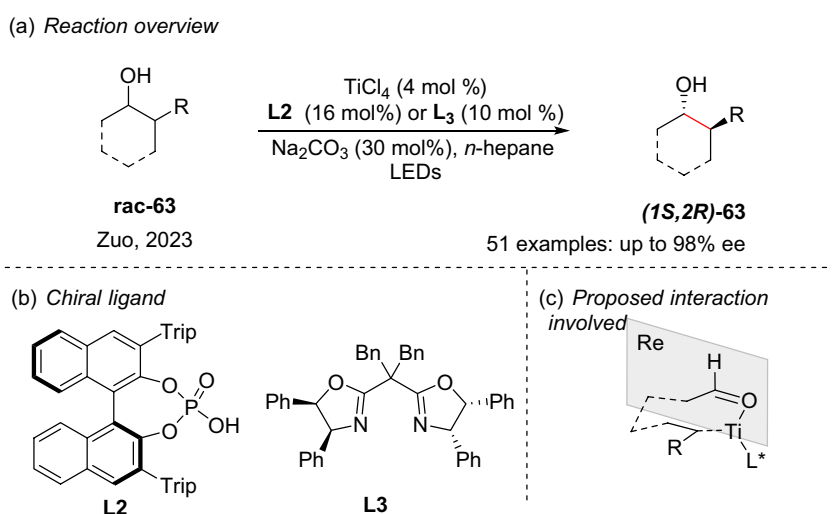
Direct activation of the Lewis acid-substrate complex has also been employed in the context of deracemization reactions. More specifically, in 2023, Gilmour and

coworkers⁵⁷ successfully achieved the Al-salen-catalyzed deracemization of acylcyclopropanes under violet light irradiation (Scheme 25). With the assistance of DFT calculations, the authors discovered that stereoselective control of the reaction did not originate from the selective recognition of the substrate, but rather from the stereospecific cyclization of the biradical intermediate produced through the ring opening of cyclopropane.

Zuo and coworkers⁵⁸ achieved deracemization of alcohols through the cleavage and stereospecific reformation



Scheme 25 | Photoinduced deracemization of cyclopropanes using chiral aluminum catalysis.

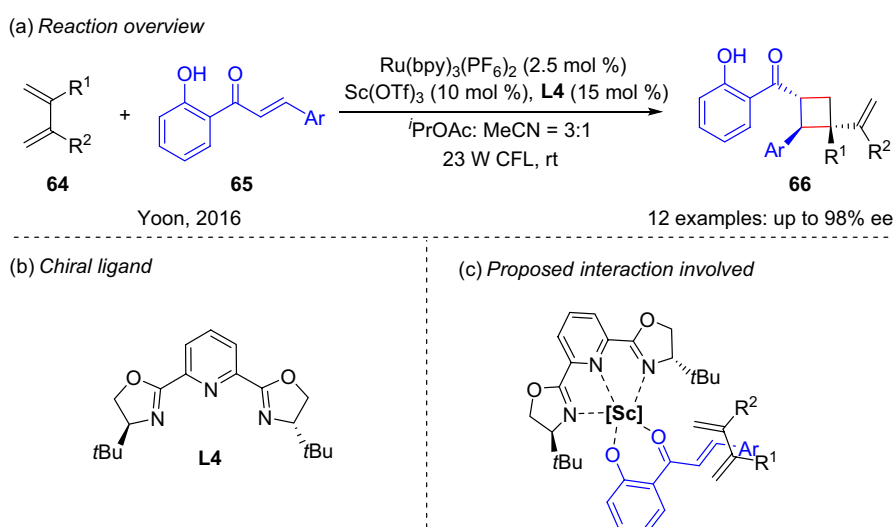


Scheme 26 | Photoinduced deracemization of alcohols using chiral titanium catalysis.

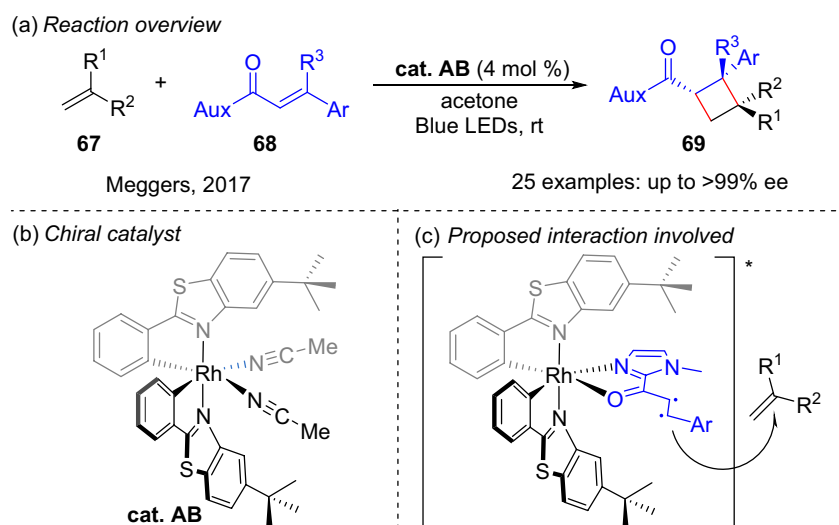
of unstrained C–C bonds via a chiral Ti-catalyzed ligand-to-metal charge transfer (LMCT) process (Scheme 26). This reaction elegantly exploits high-valent Ti(IV) catalysts as LMCT-competent Lewis acids to generate carbon-centered radicals, which are subsequently intercepted by low-valent Ti(III) species mediating asymmetric C–C bond formation. Mechanistic investigations revealed that the chiral titanium catalyst facilitated moderate stereocontrol during both the bond-breaking and bond-forming steps. Remarkably, the combination of these two moderately enantioselective events led to a multiplicative enhancement of stereoinduction. This innovative strategy achieved outstanding stereoselectivity, with enantiomeric ratios reaching up to 99:1, showcasing the power of LMCT catalysis in asymmetric synthesis.

Triplet energy transfer

It has been reported that Lewis acid-catalyzed energy transfer can offer an alternative pathway for achieving asymmetric [2+2] PCAs.⁵⁹ More specifically, the coordination of a carefully selected Lewis acid with the desired substrate can decrease the energy required for the substrate to reach its excited state. In 2016, Yoon and coworkers⁶⁰ reported an asymmetric [2+2] PCA reaction between 2'-hydroxychalcones and 1,3-dienes via a Lewis acid-catalyzed triplet energy transfer protocol (Scheme 27). Using this approach, the use of relatively complex cyclic substrates can be avoided, and chiral vinylcyclobutanes can be obtained from simple acyclic enone substrates. A dual catalytic system is established involving a Ru(bpy)₃²⁺ triplet sensitizer and an in situ



Scheme 27 | Photocatalytic asymmetric [2+2] PCA using a chiral Sc(III)-complex.



Scheme 28 | Photocatalytic asymmetric [2+2] PCA using a bifunctional chiral-at-Rh complex.

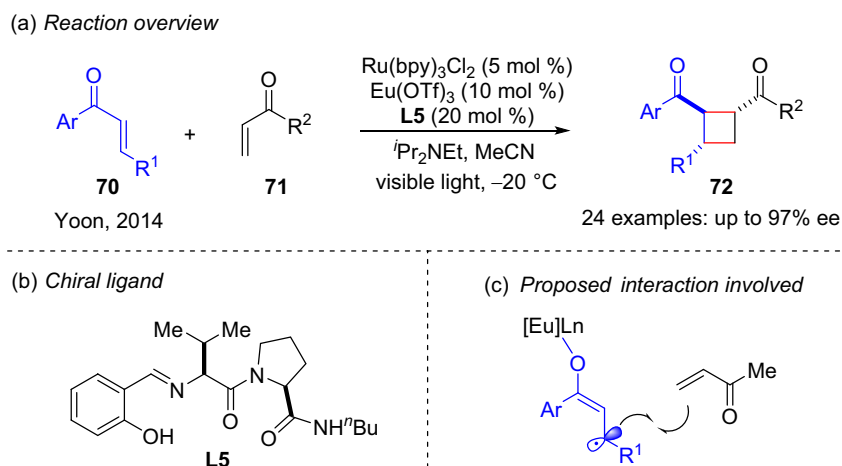
formed Sc(III)PyBox-substrate complex. Sc(III) complex coordination not only notably decreases the singlet-triplet gap of the substrate (calculated triplet energy decrease from 51 to 32 kcal/mol) but also induces the enantioselectivity of cycloadditions by choosing suitable substituents on the PyBox ligand.

In some instances, a single chiral Lewis acid is efficient enough to achieve the triplet state of the coordinated substrate, and no additional photocatalyst is necessary.⁶¹ Instead of a dual catalytic system, Meggers and coworkers⁶² disclosed a simplified method using a bis-cyclometalated chiral-at-Rh complex catalyst to produce a series of chiral cyclobutanes in yields of $\leq 95\%$ and ee values of $\leq 99\%$ (Scheme 28). This strategy takes advantage of the reactivities of photoexcited molecules to conduct direct bond-forming reactions. Following coordination with the chiral-at-Rh Lewis acid catalyst,

irradiation of the Rh-substrate complex with visible light directly generated the triplet excited state, allowing control of the reaction enantioselectivity through distinguished steric repulsion, as depicted in Scheme 28 (bottom right).

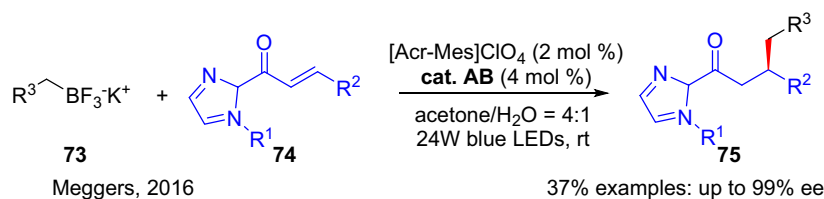
Single electron transfer

Single electron transfer is the most frequently used mode to generate reactive radical species in visible light photocatalysis.⁶⁻⁸ In asymmetric photochemical synthesis, the cooperation of chiral Lewis acids with radical intermediates or radical acceptors can manipulate the stereoselectivity of the reaction, and a large number of well-studied chiral Lewis acids are available for promoting stereochemical control in enantioselective photochemical transformations.⁵⁹ The first chiral Lewis acid/

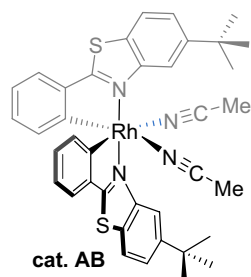


Scheme 29 | Photocatalytic enantioselective PCA using a chiral Eu-complex.

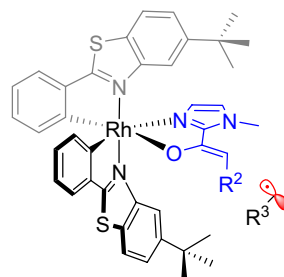
(a) Reaction overview



(b) Chiral catalyst



(c) Proposed interaction involved



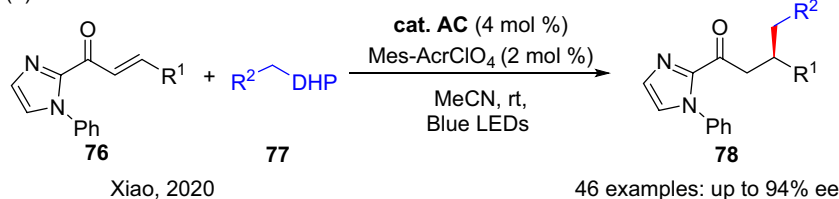
Scheme 30 | Photocatalytic enantioselective conjugate addition using a chiral-Rh complex.

photoredox catalysis system for asymmetric conjugate addition was disclosed in 2014 by Yoon (Scheme 29).⁶³ In this cyclization achieved via a dual catalysis strategy, the enone substrate is unable to absorb visible light, and so no unselective background reaction takes place in the absence of a photocatalyst or a chiral Lewis acid. Thus, using $\text{Ru}(\text{bpy})_3^{2+}$ as a photocatalyst and a chiral Eu-based Lewis acid complex to control the stereochemistry, cyclobutanes were obtained with enantioselectivities of $\leq 97\%$ ee via the corresponding [2+2] PCA process.

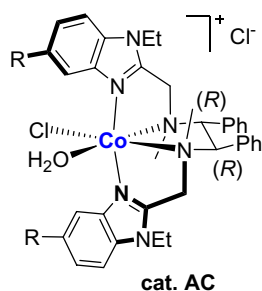
In 2016, Meggers and coworkers⁶⁴ discovered that bis-cyclometalated rhodium promoted the enantioselective

conjugate addition of nucleophilic benzyl radicals to generate rhodium enolates (Scheme 30). In this reaction, α,β -unsaturated 2-acyl imidazoles and α,β -unsaturated *N*-acyl pyrazoles are perfect substrates to coordinate with the chiral-at-Rh complex. However, an additional photocatalyst was necessary to promote the oxidative generation of benzyl radicals. Conjugate addition of the benzyl radical to an α,β -unsaturated carbonyl compound represents an enantio-determined step, which relies on steric repulsion from the *Re*- or *Si*-face of the chiral Rh-coordinated radical acceptor. It was found that a relatively low quantity of the Lewis acid catalyst was

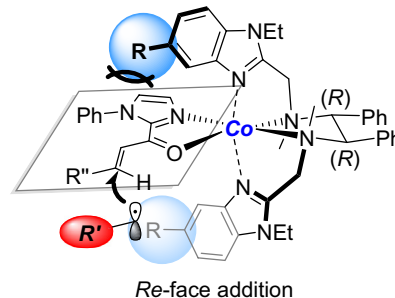
(a) Reaction overview



(b) Chiral catalyst



(c) Proposed interactions involved

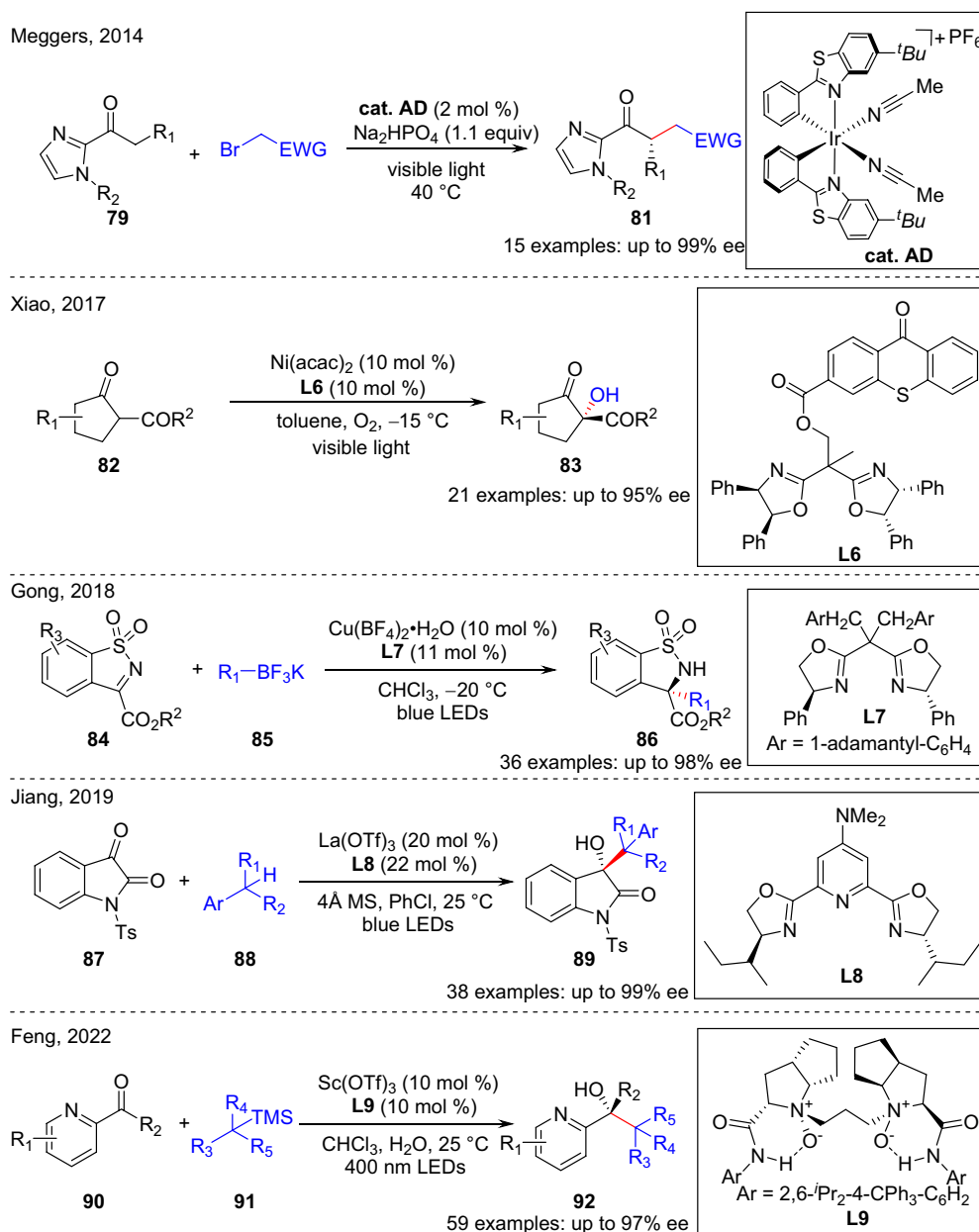


Scheme 31 | Photocatalytic asymmetric conjugate addition using a chiral cobalt complex.

sufficient to achieve a high enantioselectivity and yield, despite the remarkable background reaction.

Recent studies have shown that cobalt can be considered as a replacement for rhodium because of its similar outer electron arrangement. In 2019, Xiao and coworkers⁶⁵ realized the photocatalytic asymmetric radical conjugate addition reaction of α,β -unsaturated carbonyls with Hantzsch esters (HEs), constructing chiral carbonyl compounds through the use of sterically well-defined chiral octahedral cobalt catalysts (Scheme 31). In the stereoreduction model, the radical is added from the *Re*-surface of the activated enone due to the reduced steric hindrance from the ligand.

In addition to photocatalytic asymmetric radical addition to α,β -unsaturated systems, radical additions to enolate, iminium, and carbonyl systems have been achieved in an asymmetric fashion through asymmetric Lewis acid catalysis. As reported recently by Meggers,⁶⁶ Lu and Xiao,⁶⁷ Gong,⁶⁸ Jiang,⁶⁹ and Feng,⁷⁰ Ir-, Ni-, Cu-, La-, and Sc-based chiral complexes have been found to be highly efficient chiral Lewis acid catalysts for these transformations (Scheme 32). Although these reactions may proceed through radical addition or radical-radical coupling pathways, these chiral Lewis acids successfully activate the substrates and induce stereoselectivity.



Scheme 32 | Photocatalytic asymmetric radical additions to other acceptors using chiral Lewis acids.

Asymmetric Photocatalysis with Transition Metal Catalysis

The merging of transition metal catalysis and photochemistry has tremendous potential for the generation of organometallic intermediates and the formation of carbon-carbon/-heteroatom bonds under mild reaction conditions, which were previously believed to be difficult or impossible to achieve.⁷¹ In particular, the introduction of visible light photocatalysis or photoexcitation to asymmetric transition metal catalysis represents a new route toward chiral molecules. In this section, stereocontrol strategies in this field are highlighted in the context of different transition metals.

Visible light induced asymmetric nickel catalysis

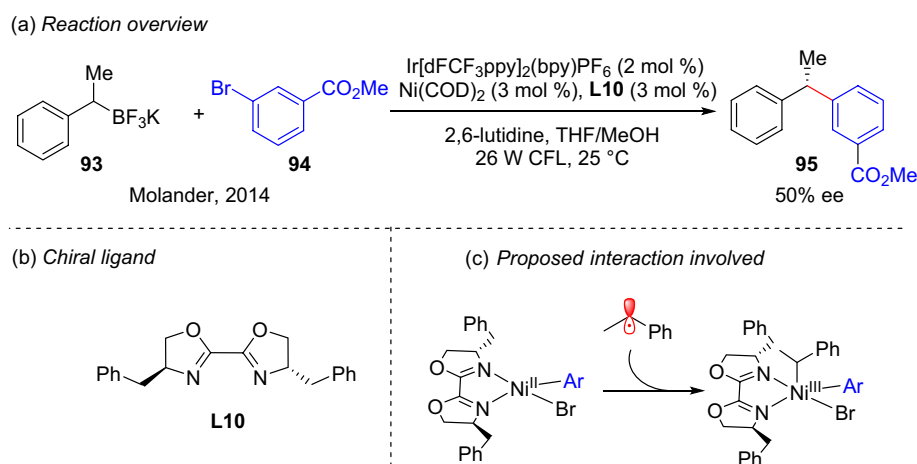
As a conventional transition metal catalyst, nickel has been employed to promote C–C bond generation via a range of cross-coupling reactions. Recently, the use of chiral ligands has also rendered the corresponding stereocontrolled transformations feasible.^{72,73} For example, in 2014, photoredox-mediated nickel-catalyzed cross-coupling reactions were reported by several groups, including those of Molander⁷⁴ and MacMillan.⁷⁵ Their works represented pioneered research into the merging of photoredox catalysis and nickel catalysis for C(sp²)-C(sp³) coupling reactions. The first such example was reported by Molander and coworkers (Scheme 33).⁷⁴ Using a commercially available chiral bisoxazoline ligand, the cross-coupling reaction between a racemic trifluoroborate and an aryl bromide exhibited a moderate enantioselectivity (50% ee), thereby demonstrating the possibility of stereocontrol in asymmetric photocatalysis.

Later, Fu et al. reported a successful combination of asymmetric Ni-catalyzed cross-coupling with a

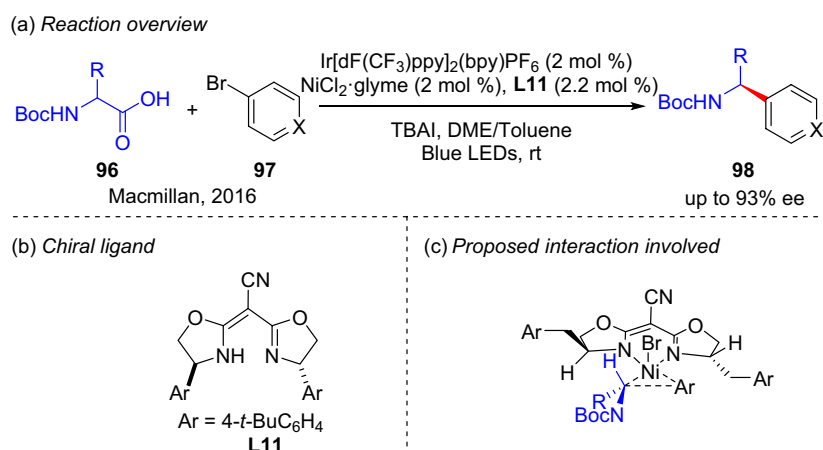
metallaphotoredox-mediated decarboxylative arylation protocol (Scheme 34),⁷⁶ wherein a diverse set of *N*-Cbz- and *N*-Boc-protected amino acids was applied as radical precursors to couple with readily available aryl halides. By exploiting the chiral cyano-BOX (bisoxazoline) ligand, the corresponding benzylic amine products were obtained in enantioselectivities of $\leq 93\%$. As key intermediates, alkyl radicals were generated during the photocatalytic cycle through reductive quenching. Simultaneously, chiral aryl Ni(II) species were formed via oxidative addition. Notably, this work constitutes the first one-step synthesis of highly enantioselective benzylic amines via a photoredox catalytic cycle, which is also the first enantioselective metallaphotoredox reaction that has demonstrated satisfactory stereogenic control.

In 2017, Doyle and coworkers realized a nickel/photoredox catalytic desymmetrization of cyclic carboxylic anhydrides with organotrifluoroborates (Scheme 35),⁷⁷ wherein highly enantioselective keto-acid products were obtained with good functional group tolerance. It was found that chiral BOX ligands exhibited excellent stereocontrol in this transformation ($\leq 91\%$ ee). Furthermore, it was suggested that this enantioselectivity was established during the initial oxidative addition of the low-valence Ni catalyst to the symmetric cyclic carboxylic anhydride, and that the singlet electron oxidation of Ni(II) to Ni(III) may accelerate the subsequent reductive elimination step.

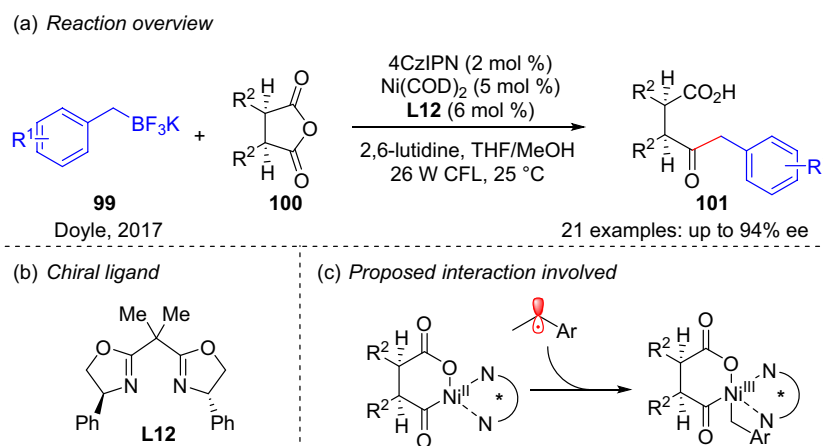
In subsequent years, asymmetric photo/nickel catalysis emerged as a rapidly developing and effective tool for constructing chiral carbon-carbon bonds (Scheme 36). Indeed, significant progress has been made in the asymmetric α -arylation of diverse functional groups, encompassing carbonyl,⁷⁸ aryl,⁷⁹ ester,⁸⁰ borate,⁸¹ trifluoromethyl,⁸² phosphonyl,⁸³ and ether groups,⁸⁴ among others. Furthermore, the asymmetric migratory insertion of carbon-nickel bonds into intramolecular olefins,



Scheme 33 | First example of a Ni-catalyzed photoredox enantioconvergent cross-coupling reaction.



Scheme 34 | Nickel-catalyzed photoredox enantioconvergent decarboxylative arylation.



Scheme 35 | Nickel-catalyzed photoredox enantioselective desymmetrization reaction.

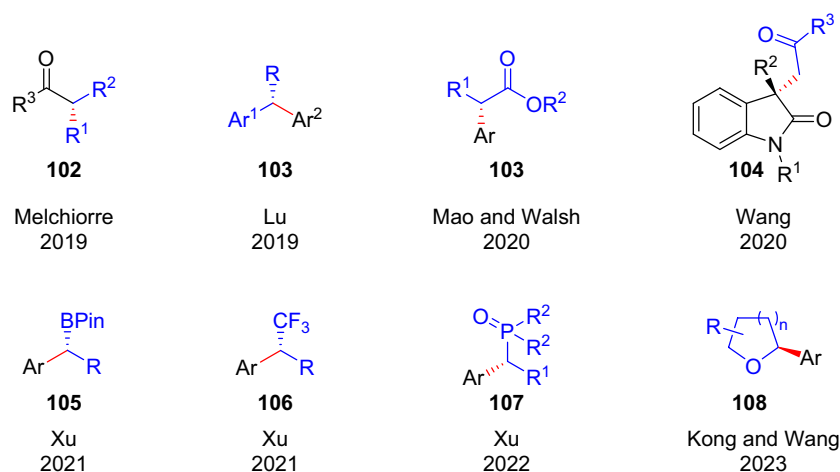
followed by their coupling with photogenerated radicals, has been validated as a potent approach for the synthesis of chiral oxidized indoles.⁸⁵

Visible light induced asymmetric copper catalysis

The combination of photocatalysis and copper catalysis offers an alternative approach for achieving stereoselective transformations.⁸⁶ For example, in 2016, Fu and coworkers⁸⁷ reported an elegant strategy to trigger visible light-induced asymmetric C–N cross-coupling reactions using a single chiral copper–phosphine catalyst (Scheme 37). No exogenous photocatalyst was required in this reaction, although a chiral phosphine ligand was necessary to produce the photoresponsive copper complex and achieve good stereocontrol. Upon excitation of the copper–nucleophile complex by visible light, C–X bond cleavage is promoted through SET, achieving a

wide range of C–N cross-coupling products in high enantioselectivities. Subsequent mechanistic experiments revealed that the chiral C–N bond was directly formed through an interaction between the coordinated carbonyl α -radical and the Cu(II)-bound carbazole N atom, rather than via an alkyl Cu(III) intermediate.⁸⁸

In 2017, Liu and coworkers⁸⁹ investigated the viability of the asymmetric decarboxylation reactions between *N*-hydroxyphthalimide esters and trimethylsilyl cyanide via dual photoredox/copper catalysis (Scheme 38). Under mild conditions, the use of chiral bis(oxazoline) ligands facilitated the efficient synthesis of a range of enantiomerically enriched benzyl nitriles ($\leq 99\%$ ee), encompassing various key chiral intermediates for the preparation of bioactive compounds. DFT calculations were also employed to investigate the energy barriers associated with the reaction transition states, revealing that the addition of benzyl radicals to Cu(II) to generate Cu(III) has a slightly lower energy barrier than the reductive



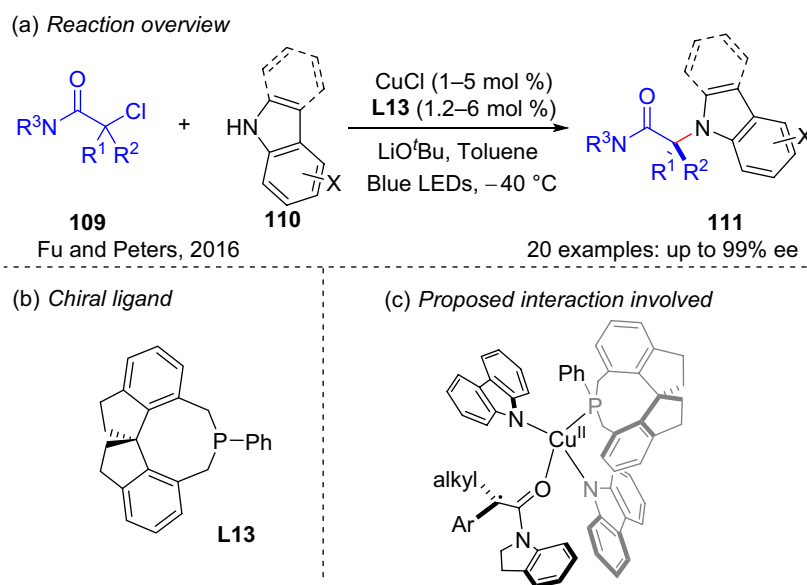
Scheme 36 | Examples of products generated via nickel-catalyzed photoredox enantioselective cross-coupling reactions.

elimination step. The addition of radicals to Cu(II) is postulated to be a reversible process, whereas the ultimate reduction–elimination step serves as the key determinant of the reaction enantioselectivity.⁹⁰

The direct asymmetric C–H amination reaction for the production of chiral β -amino alcohols is notable due to the challenge of achieving both enantioselectivity and regioselectivity in the same protocol (Scheme 39).⁹¹ Recently, an elegant methodology was developed by Nagib and coworkers,⁹¹ providing chiral β -amino alcohols via a radical relay strategy. The chiral catalyst participates in the radical generation step and terminates the radical event, creating an ideal chiral environment for the variant.

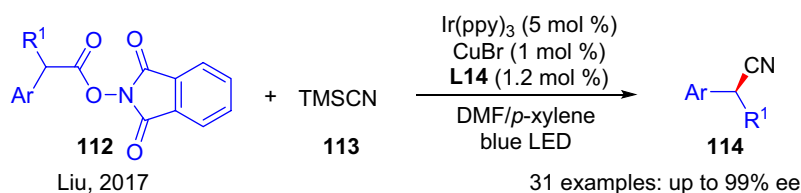
Compared with nickel catalysis, synergistic light/copper catalysis boasts a more extensive array of nucleophilic reagents, including cyano,^{92,93} alkynyl,^{94,95} aryl,⁹⁶ heteroaryl,⁹⁷ amide,⁹⁸ carboxylic acid,⁹⁹ trifluoromethyl,¹⁰⁰ and alkyl compounds¹⁰¹ (Scheme 40). Furthermore, its reaction sites exhibit a greater versatility, including the propargyl, allyl, benzyl positions, as well as the α -positions of esters and amides. Notably, copper catalysis can also address the challenging task of constructing chiral quaternary carbon centers.¹⁰²

Ultraviolet (UV)-induced Cu-catalyzed olefin isomerization is an effective method for the production of Z-olefins.¹⁰³ However, the use of high-energy UV light poses challenges for achieving stereoselective control

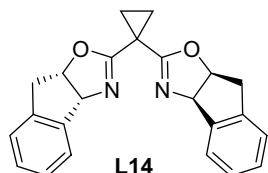


Scheme 37 | Copper-catalyzed photoredox enantioconvergent cross-coupling reaction.

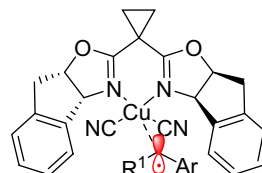
(a) Reaction overview



(b) Chiral ligand

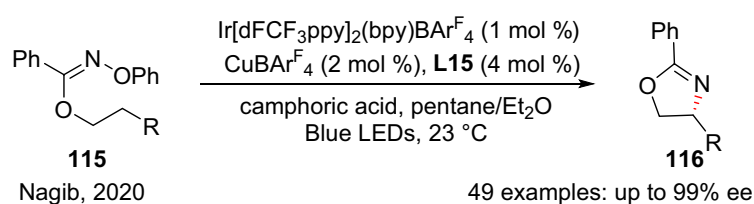


(c) Proposed interaction involved

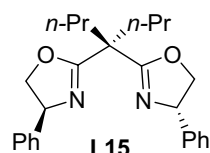


Scheme 38 | Copper-catalyzed photoredox enantioconvergent decarboxylative cyanation.

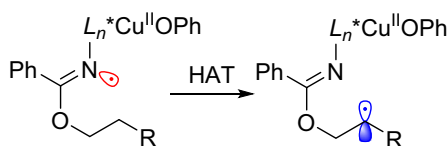
(a) Reaction overview



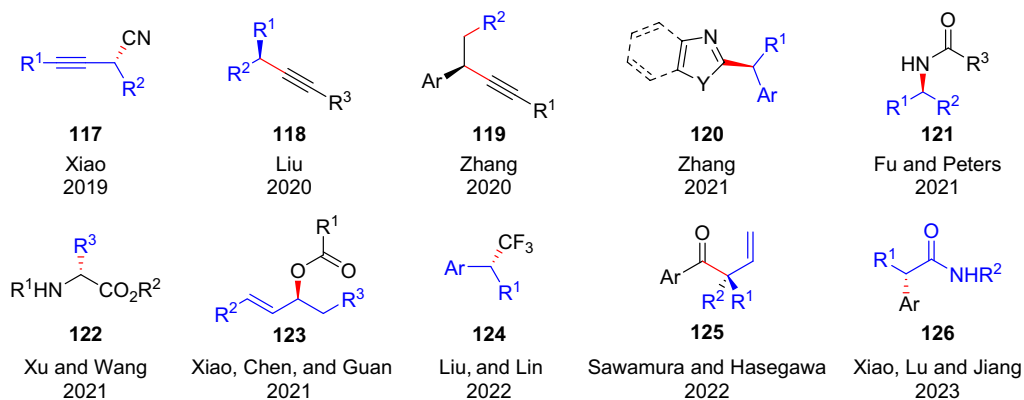
(b) Chiral ligand



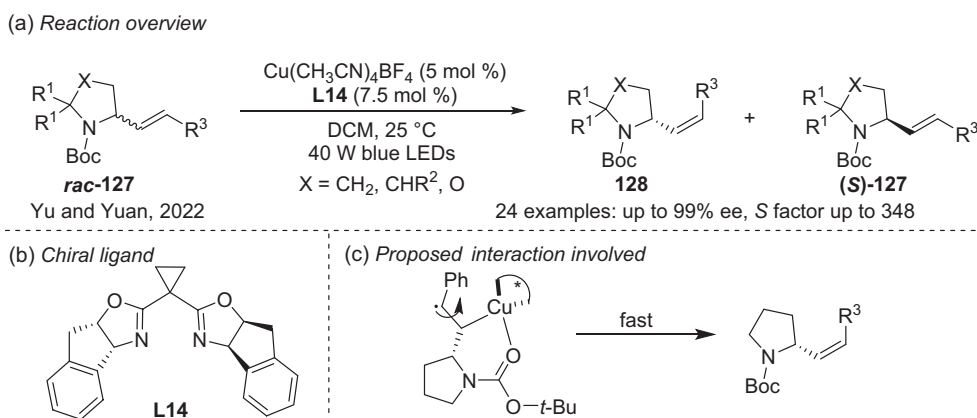
(c) Proposed interaction involved



Scheme 39 | Copper-catalyzed photoredox enantioconvergent amination of alcohols.



Scheme 40 | Examples of copper-catalyzed photoredox enantioconvergent cross-coupling reactions.



Scheme 41 | Copper-catalyzed kinetic resolution of alkene via photoisomerization.

during this process. In 2022, Yu and coworkers¹⁰⁴ employed racemic 2-styrylpyrrolidine derivatives as substrates and developed a strategy that leverages photoexcited chiral copper complexes to mediate the enantioselective *E/Z* isomerization and successfully facilitated kinetic resolution (Scheme 41). Notably, this method has been applied in the total synthesis of two enantiomers of the bioactive indolizidine alkaloid 201. DFT calculations revealed that the *R*-configured pyrrolidine substrate formed a more stable complex with the catalyst in the ground state, which was attributed to coordination between the carbonyl oxygen atom and the copper center. Furthermore, this O–Cu interaction reduces the electronic activation energy required for the *R*-configuration substrate to overcome the single-bond rotation segment, resulting in a higher photosensitization efficiency. This difference in sensitization rates enables the efficient achievement of kinetic resolution processes.

Visible light induced asymmetric chromium catalysis

Stoichiometric chromium reagents have been described as highly efficient catalysts in the venerable Nozaki–Hiyama–Kishi (NHK) alkylation reaction.¹⁰⁵ Recently, novel strategies toward the catalytic asymmetric NHK allylation of aldehydes have appeared due to the pioneering work of Glorius, who ingeniously combined asymmetric chromium catalysis with visible light photocatalysis.¹⁰⁶ During this process, the crucial allyl chromium species is generated in situ via a photoredox catalysis cycle. Although the substrate scope is limited to allyl amines and arenes, an intriguing asymmetric outcome was obtained using a chiral carbazole-based BOX ligand, giving a moderate enantiomeric excess of the desired product (20% ee). Encouraged by this interesting result, the same group utilized readily available 1,3-dienes via similar mechanistic pathways to expand the reaction scope. Consequently, they demonstrated that

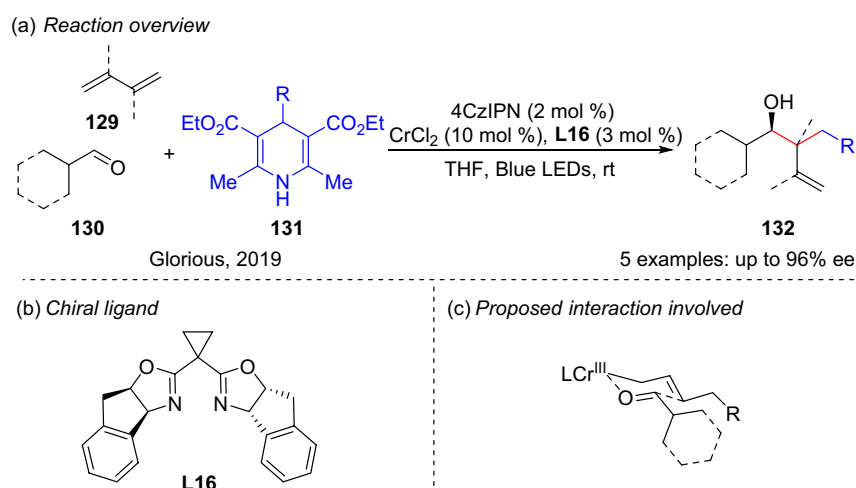
enantioenriched homoallylic alcohols ($\leq 96\%$ ee) can be produced in a single reaction from aldehydes, alkenes, and HEs using a chiral chromium BOX complex (Scheme 42).¹⁰⁷

In 2024, Wang and coworkers¹⁰⁸ successfully achieved the asymmetric addition of α -amino radicals to aldehydes, leveraging the synergistic effects of photoredox reactions, HAT, and chromium catalysis (Scheme 43). This innovative approach efficiently yields chiral β -amino alcohol compounds, wherein the Cr catalyst effectively governs the stereoselectivity of the reaction. Additionally, the quinone ring serves as a HAT reagent, selectively cleaving the α -C–H bond of the amine group to generate α -amino radicals. Notably, the captured hydrogen atoms also facilitate dissociation of the Cr–O bond. DFT calculations revealed that the direct radical addition reaction of Cr(II)/**L17**-coordinated aldehydes was more favorable than that of the cyclic transition state. Furthermore, the remarkable stereoselectivity was attributed to the steric hindrance imposed by the quinone ring and the BOX ligand.

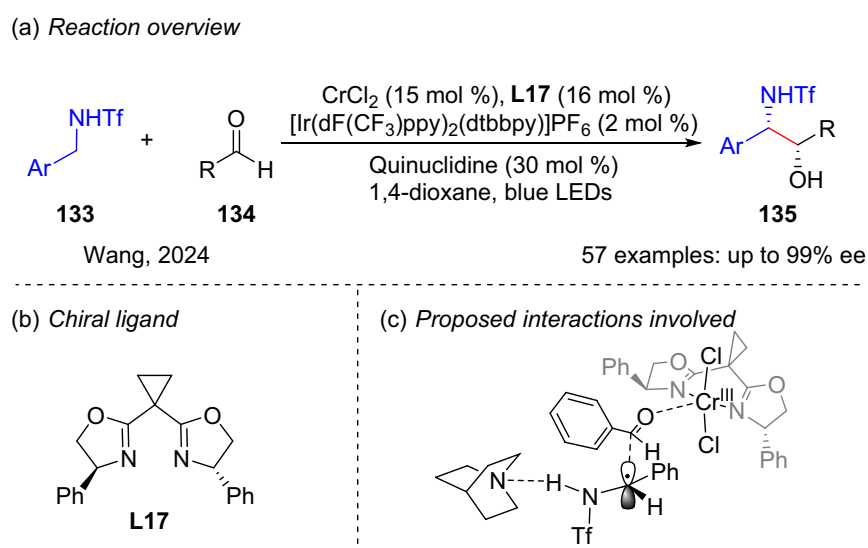
Visible light induced asymmetric cobalt catalysis

In 2021, Xia and coworkers¹⁰⁹ reported the asymmetric reductive alkenylation of aldehydes with alkynes, affording chiral allyl alcohols with high enantioselectivities via dual photoredox and asymmetric cobalt catalysis (Scheme 44). In this approach, organic reducing agents (HEs) were employed to replace the standard metal reducing agents, thereby rendering the reaction conditions milder and greener. The coordination mode of the equatorial alkyne molecule and the aldehyde with its *Re*-face pointing toward the axial position of the Co(I) center determine the stereoselectivity of the reaction.

The nucleophilic characteristics of organic cobalt intermediates can also be exploited to achieve asymmetric transformations. For example, in 2022, Xiao and



Scheme 42 | Asymmetric allylations of aldehydes via photoredox and chromium catalysis.



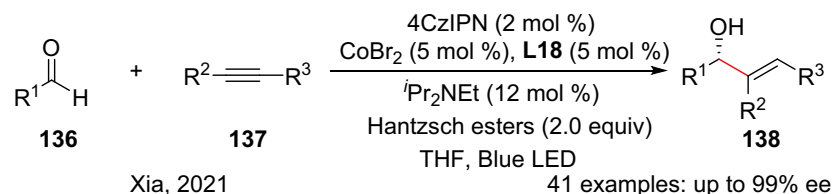
Scheme 43 | Asymmetric addition of aldehydes via photoredox and chromium catalysis.

coworkers¹¹⁰ successfully demonstrated the asymmetric reduction of aryl iodides with aldehydes via visible light-induced cobalt catalysis, affording chiral benzyl alcohols in high yields and enantioselectivities while circumventing the generation of substantial metal waste and the necessity for precious metal catalysts (Scheme 45). Furthermore, this methodology was effectively extended to the synthesis of chiral amino alcohols and D-Cloperastine. Drawing insights from the single-crystal structure of the cobalt catalyst and the absolute configuration of the product, the authors proposed a plausible stereochemical control model, highlighting the pivotal role of steric hindrance between the ligand methyl group and the axially coordinated aldehyde in governing the enantioselectivity. Furthermore, this strategy was successfully

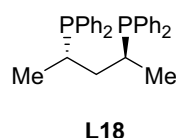
employed for the synthesis of axially chiral aldehydes via desymmetrization.¹¹¹

The axially chiral scaffold arising from rotational constraints serves as a prevalent structural motif in natural products, chiral drugs, and materials, and constitutes a crucial component of the chiral reagents, ligands, and catalysts employed in asymmetric synthesis. Nevertheless, the inherent flexibility of this scaffold poses a significant challenge for controlling the reaction enantioselectivity. In 2022, Xiao and coworkers¹¹² made a groundbreaking advancement by developing a visible light-induced asymmetric cobalt-catalyzed radical coupling reaction (Scheme 46). This reaction enables the dynamic kinetics of asymmetric racemic heteroaryl compounds, facilitating the synthesis of a diverse array of

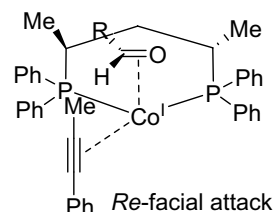
(a) Reaction overview



(b) Chiral ligand



(c) Proposed interactions involved



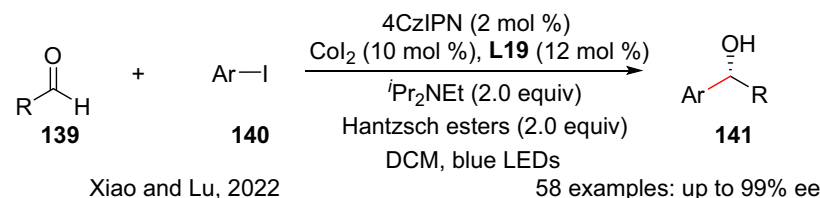
Scheme 44 | Photocatalytic asymmetric reductive couplings using a chiral cobalt complex.

axially chiral heteroaryl compounds with remarkable enantioselectivities. The crux of this reaction is the formation of axially chiral aryl cobalt species following oxidative addition, which reduces the rotational energy barrier of the axis because of the coordinating effect of pyridine, thereby facilitating racemization. Subsequently, the radicals generated by photocatalysis are captured in a stereoselective manner. In 2023, the same group expanded this strategy to successfully achieve a synergistic visible light/cobalt catalytic process that promoted an asymmetric reduction conjugate addition reaction with dynamic kinetics.¹¹³

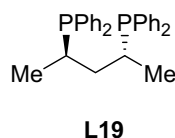
Cobalt-catalyzed asymmetric C–H bond activation has been successfully implemented for the efficient

construction of both central and axial chiralities, wherein the incorporation of photocatalysts was expected to eliminate the requirement for stoichiometric metal oxidants. In 2024, Shi and coworkers¹¹⁴ achieved the asymmetric dearomatization of indole via a photoassisted cobalt-catalyzed enantioselective C–H bond functionalization protocol (Scheme 47). Based on the single-crystal structure of the Co(II)/salox complex, the authors discovered that the π – π interaction between the phenyl group of the oxazoline ligand and the quinoline moiety of the substrate facilitated the precise establishment of cobalt chirality and the formation of a hand cavity that binds with indole. Further mechanistic studies revealed that visible-light irradiation facilitated the

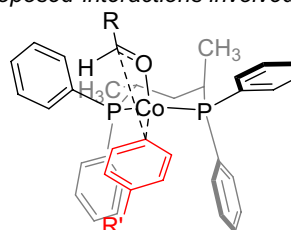
(a) Reaction overview



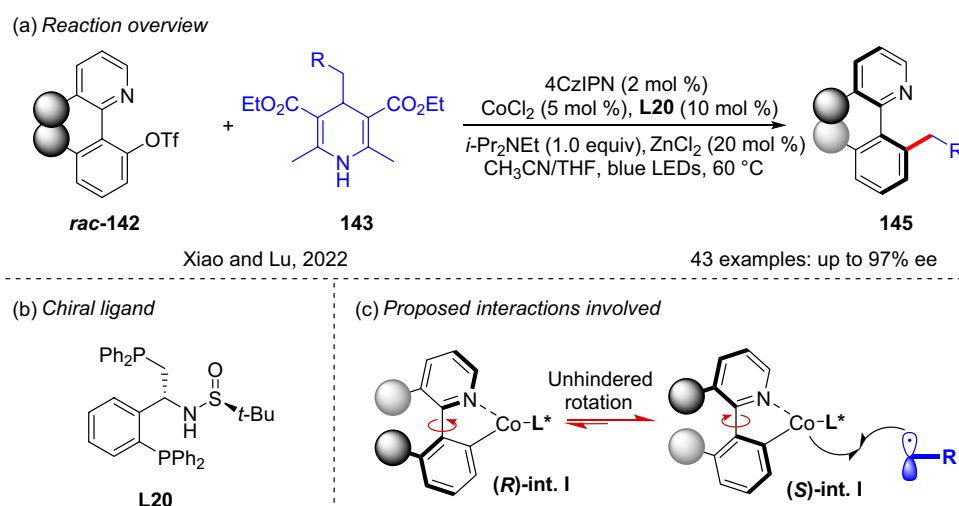
(b) Chiral ligand



(c) Proposed interactions involved



Scheme 45 | Photocatalytic asymmetric reductive Grignard-type addition using a chiral cobalt complex.



Scheme 46 | Photocatalytic construction of axial chirality using a chiral cobalt complex.

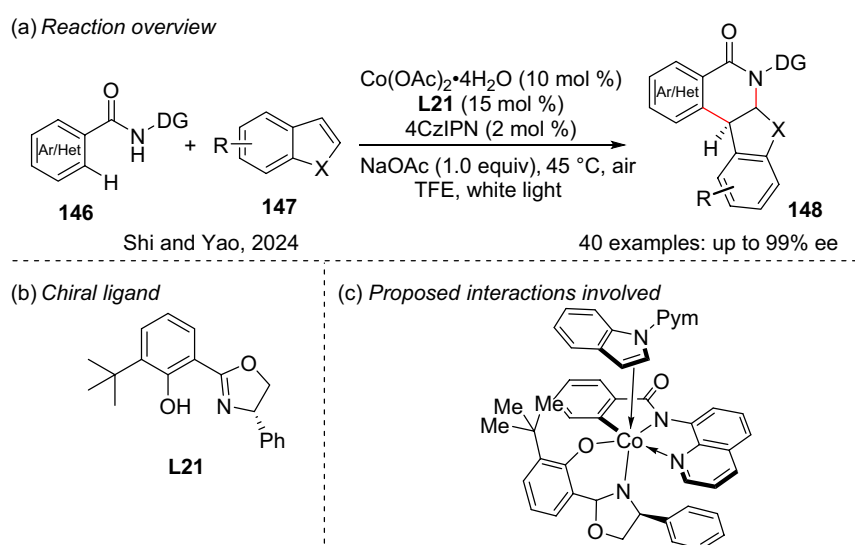
migratory insertion of the C-Co(III) bond during dearomatization.

Visible light induced asymmetric palladium and iridium catalysis

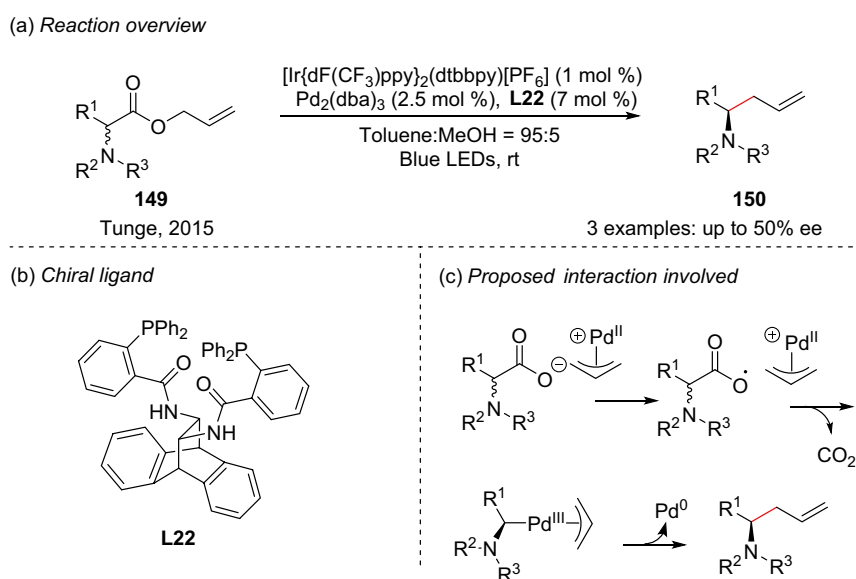
Transition metal-catalyzed allylic substitution reactions, especially those involving the use of palladium and iridium, are powerful tools for the selective construction of chemical bonds.¹¹⁵ Recently, the introduction of excited-state chemistry has significantly expanded the scope of this methodology due to the important contributions from Tunge, Lu, and Xiao.^{116,117} Notably, the first example merging asymmetric palladium catalysis and visible light photocatalysis was carried out by Tunge and

coworkers,¹¹⁸ wherein the corresponding product was obtained in a moderate enantioselectivity via the decarboxylative allylation of *N*-protected amino esters with a chiral Trost ligand (Scheme 48). In the presence of a *N*-Boc-amino ester, which generates a less stable amino radical, a relatively higher enantiomeric excess (50% ee) was obtained compared to those achieved using more stable amino radicals (~0% ee). This interesting result confirms the participation of the chiral palladium complex in the asymmetric C-C bond-forming step, and highlights the importance of employing a suitable chiral ligand in asymmetric dual palladium/photoredox catalysis.¹¹⁷

Later, a breakthrough in this area was achieved by Yu and coworkers,¹¹⁹ who accomplished a general



Scheme 47 | Photocatalytic enantioselective C-H functionalization using a chiral cobalt complex.



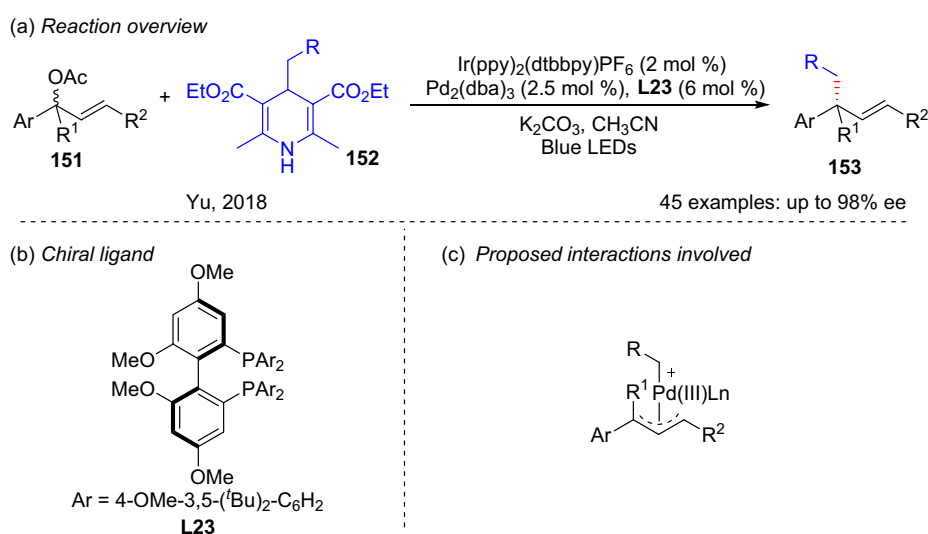
Scheme 48 | Palladium-catalyzed photoredox asymmetric cross-coupling reaction with linear selectivity.

asymmetric radical allylation reaction of 4-alkyl Hantzsch esters (HZs) using electron-rich chiral biphosphine ligands (Scheme 49). In contrast to the work by Tunge et al.,¹¹⁸ this allylation alkylation exhibited good branched selectivity, which may be related to the unknown reactivity and selectivity of the Pd(III) species in the reductive elimination step. Simultaneously, the stereoselectivity of the allyl position was well controlled by stereoreduction from chiral biphosphine ligand **L23**.

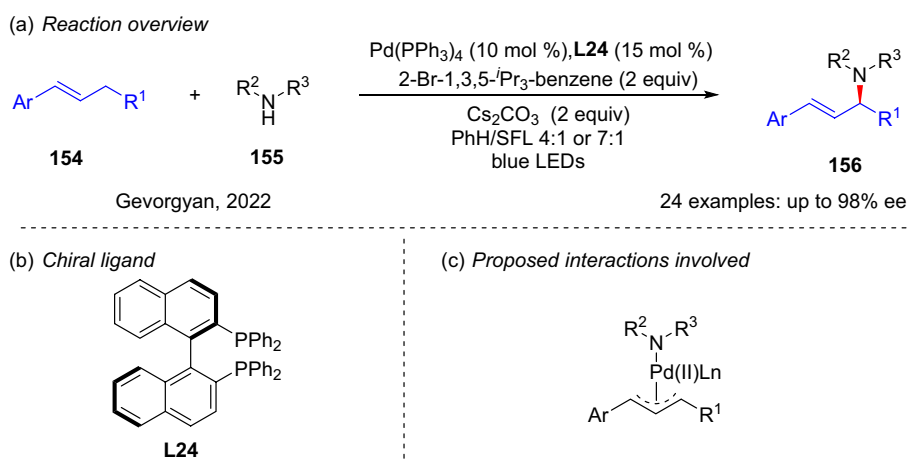
With the advancement in cooperative photoredox/palladium catalysis, Pd(I) intermediates have attracted significant attention. In 2022, Gevorgyan and coworkers¹²⁰ reported the intermolecular asymmetric

C-H bond amination of various substituted olefins with primary/secondary aliphatic amines using a photoinduced Pd(O/I/II) catalytic strategy (Scheme 50). Notably, the Pd(I) intermediate, which was generated via photoinduced homolytic cleavage, attenuated the Lewis acidity of the system, ultimately minimizing olefin isomerization, and reducing the degree of interaction between the catalyst and the amine.

In 2024, Yu and coworkers¹²¹ developed a strategy involving visible light-excited palladium catalysis, and successfully performed a series of deracemization reactions to generate racemic dienes (Scheme 51). Theoretical calculations revealed that in the ground state, the



Scheme 49 | Palladium-catalyzed photoredox asymmetric cross-coupling reaction with branched selectivity.



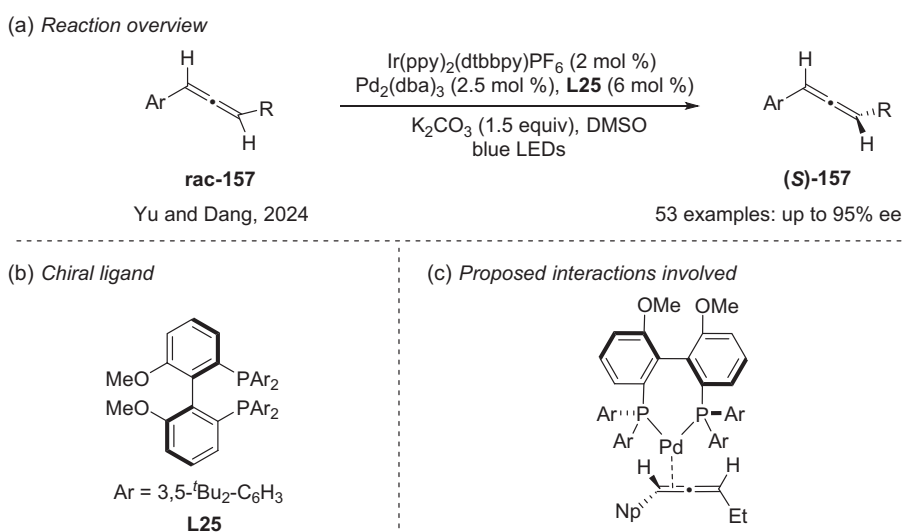
Scheme 50 | Palladium-catalyzed photoredox allylic C–H amination of alkenes.

$\text{Pd(O)}\text{-}R_{\text{SO}}$ complex possessed a lower energy and exhibited a reduced vertical excitation energy owing to steric repulsion between the ligand and the substrate. Upon excitation, the $\text{Pd(I)}\text{-}S_{\text{T}_1}$ complex, whose substrate ligand exhibits a stronger dispersive attraction, underwent conversion from $\text{Pd(I)}\text{-}R_{\text{T}_1}$ to $\text{Pd(I)}\text{-}S_{\text{T}_1}$. Furthermore, the introduction of K_2CO_3 into the reaction system enhanced the $\pi\text{-K-}\pi$ interactions in the $\text{Pd(I)}\text{-}S_{\text{T}_1}$ system compared to those in the $\text{Pd(I)}\text{-}R_{\text{T}_1}$ system, thereby amplifying the energy difference in the excited state, and ultimately enhancing the overall stereoselectivity.

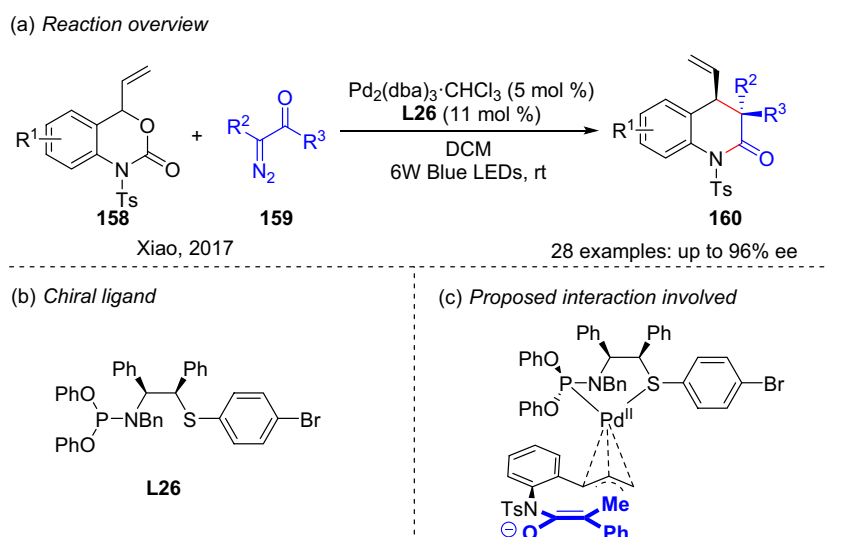
Although ketenes are appealing chemicals for the construction of valuable chiral heterocycles via asymmetric $[n+2]$ cycloaddition protocols,¹²² they have not been exploited well in low-valence transition-metal catalysis because of their inherent electron-deficient properties (Scheme 52). Xiao and coworkers¹²³ overcame this

challenge by introducing a photoinduced Wolff rearrangement to promote the in situ formation of reactive ketenes from α -diazoketones. In this system, vinyl benzoxazinones are activated by a chiral Pd(O) catalyst to generate 1,4-dipolar intermediates, which can be stereoselectively captured by the slowly released ketenes. Consequently, the asymmetric synthesis of highly enantiopure quinolinones via sequential Wolff rearrangement/palladium catalysis was realized in a 99% yield and a $\leq 96\%$ ee. The carefully designed P,S ligand exhibited a high stereocontrol and slowed decomposition of the ketene/diazo compound in the presence of the palladium catalyst.

Compared with base-state palladium catalysis, the iridium-catalyzed allylation reaction demonstrates a superior branched selectivity, rendering it easier to control the allyl site chirality.¹²⁴ Recently, Melchiorre and coworkers¹²⁵ used simple allyl alcohols and 4-aminoalkyl-substituted



Scheme 51 | Palladium-catalyzed photoredox deracemization of allenes.



Scheme 52 | Palladium-catalyzed asymmetric (4+2) cycloadditions with photogenerated ketenes.

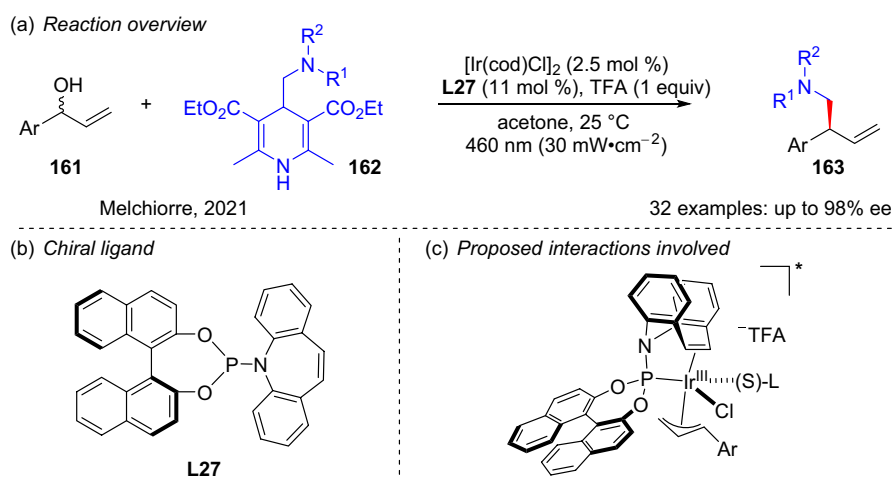
HZs as substrates to develop a photoexcited iridium-catalyzed asymmetric allylation reaction, successfully constructing C(sp³)-C(sp³) bonds with high enantioselectivity (Scheme 53). Significant experimental evidence shows that the chiral allyl-Ir(III) complex can reach an excited state under blue light irradiation, enabling a stronger single electron transfer ability. The enantioselectivity was effectively induced by use of the Carreira ligand, which is commonly employed in a wide range of Ir-catalyzed asymmetric allylic substitutions.¹²⁶ This novel light excitation mode further expands the potential of combined light/transition metal catalysis.

In 2023, You and coworkers¹²⁷ successfully achieved the asymmetric synthesis of chiral cyclobutane derivatives through an iridium-catalyzed asymmetric allyl etherification protocol coupled with a [2+2] photocycloaddition cascade (Scheme 54). This reaction

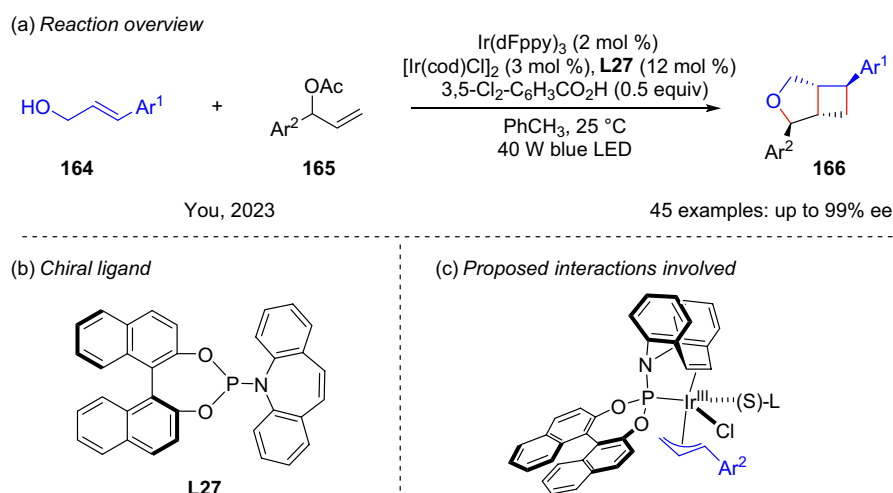
employed cinnamyl alcohol as the nucleophile and branched allyl acetate as the electrophile. Under the synergistic action of iridium catalysis and visible light irradiation, chiral cyclobutane derivatives were efficiently obtained in excellent yields, diastereoselectivities, and enantioselectivities. Control experiments showed that the enantioselectivity was established during the iridium-catalyzed allyl etherification step, whereas the subsequent non-enantioselective nature of the photocycloaddition was attributed to the chirality of the substrate.

Visible light induced other metal catalysis

Iron-catalyzed C-H bond insertion is one of the most efficient methods for the synthesis of amine compounds.¹²⁸ However, the corresponding asymmetric transformations have rarely been reported because of



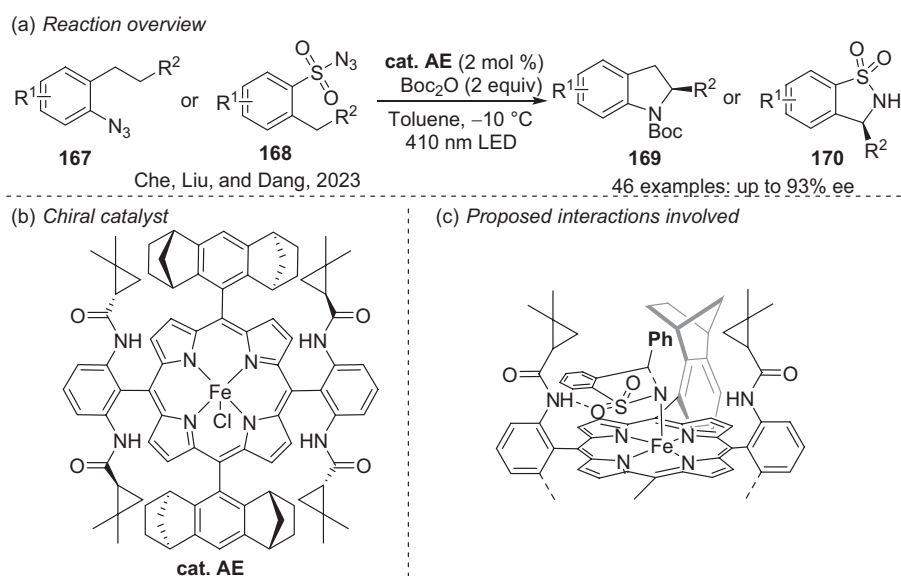
Scheme 53 | Iridium-catalyzed asymmetric cross-coupling reaction via photoexcitation.



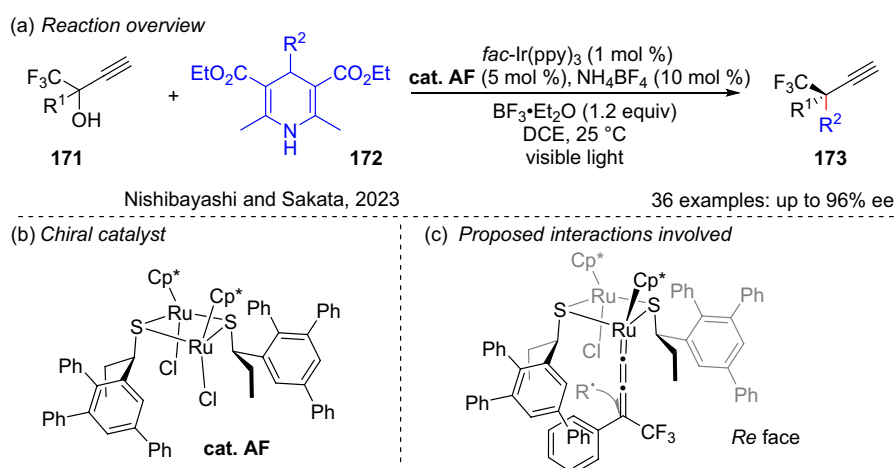
Scheme 54 | Cascade reaction involving iridium-catalyzed asymmetric allyl etherification and [2+2] photocycloaddition.

the limitations of chiral ligands in this context. In 2023, Che and coworkers¹²⁹ synthesized chiral iron complexes based on *meso*- and β -substituted porphyrins for use in the asymmetric C(sp³)-H amination of aryl and arylsulfonamide azides under visible light irradiation (Scheme 55). Mechanistic studies revealed that the iron-nitrene intermediate, generated in situ under photochemical conditions, interacts with the C(sp³)-H bond through a stepwise HAT/radical rebound mechanism. The good enantioselectivity of this process was attributed to synergistic noncovalent interactions between the iron-nitrene units and the substituents surrounding the chiral porphyrin scaffold.

Finally, in 2023, Nishibayashi and coworkers¹³⁰ reported the first example of a diruthenium-catalyzed photoinduced asymmetric propargyl alkylation reaction. They successfully synthesized a chiral terminal alkyne product with a quaternary carbon center using 4-alkyl-1,4-dihydropyridines as alkyl radical precursors and trifluoromethyl-substituted propargyl alcohol as the substrate (Scheme 56).¹³⁰ DFT calculations unveiled the existence of intramolecular π - π and C-H/F interactions among the allenylidene, optically active thiolate, and pentamethylcyclopentadienyl ligands within the diruthenium-allenylidene complex. Subsequently, the alkyl radicals predominantly interact with the *Re* face of the



Scheme 55 | Iron-catalyzed asymmetric amination of C(sp³)-H bonds via photoexcitation.



Scheme 56 | Ru-catalyzed asymmetric propargylic alkylation via photoexcitation.

diruthenium–allenylidene complex, ultimately facilitating the formation of the (*R*)-isomer as the major product.

Conclusion

In summary, this review highlights various stereocontrol strategies in the emerging field of asymmetric organic photochemical reactions, the majority of which are driven by visible light. Following a detailed analysis of these impressive advances, it was apparent that in the majority of catalytic asymmetric reactions, catalyst design is still based on an understanding of thermal reactions, leading to the stereoselectivity of the radical receptors being easy to control. In contrast, chirality control remains a challenge in radical species owing to their high reactivity and a lack of effective chiral catalysts. To date, the majority of studies have focused on the construction of chiral carbon centers, indicating the necessity to develop novel strategies for the construction of axial, planar, and topological chirality. Additionally, the construction of chiral heteroatoms (e.g., nitrogen, sulfur, and phosphorus) has yet to be addressed. Considering the various asymmetric photochemical transformations described in this review, it is noted that the majority have been applied in the large-scale syntheses of chiral chemicals for drug production, such as in the case of asymmetric thermal reactions. Visible light-induced asymmetric catalysis therefore possesses great potential for development. Ultimately, the aim of this review is to inspire researchers to engage in this field and jointly promote the role of visible light in asymmetric catalysis.

Conflict of Interest

The authors declare no competing financial interest.

DOI: 10.31635/ccschem.025.202505512
 Citation: *CCS Chem.* **2025**, *7*, 1597–1602
 Link to VoR: <https://doi.org/10.31635/ccschem.025.202505512>

Funding Information

We are grateful to the National Natural Science Foundation of China (grant nos. 92256301, 22271113, and 22471089) and National Key R&D Program of China (grant nos. 2024YFA1509700 and 2023YFA1507203).

Acknowledgments

We also thank Prof. Jia-Rong Chen and Associate Prof. Ying Cheng for helpful discussion.

References

- Zhou, Q.-L. *Chiral Materials Chemistry*; Science Press: China, **2020**.
- The Nobel Prize in Chemistry 2001. <https://www.nobel-prize.org/prizes/chemistry/2001/summary/>
- The Nobel Prize in Chemistry 2021. <https://www.nobel-prize.org/prizes/chemistry/2021/summary/>
- Jacobsen, E. N.; Pfaltz, A.; Yamamoto, H. *Comprehensive Asymmetric Catalysis*; Springer-Verlag: Germany, **2003**.
- Ding, K.-L.; Fan, Q.-H. *Asymmetric Catalysis: New Concepts and Methods*; Chemical Industrial Press: China, **2009**.
- Schultz, D. M.; Yoon, T. P. Solar Synthesis: Prospects in Visible Light Photocatalysis. *Science* **2014**, *343*, 1239176.
- Prier, C. K.; Rankic, D. A.; MacMillan, D. W. C. Visible Light Photoredox Catalysis with Transition Metal Complexes: Applications in Organic Synthesis. *Chem. Rev.* **2013**, *113*, 5322–5363.
- Karka, M. D.; Porco, J. A.; Stephenson, C. R. J. Photochemical Approaches to Complex Chemotypes: Applications in Natural Product Synthesis. *Chem. Rev.* **2016**, *116*, 9683–9747.
- Zhou, Q.-Q.; Zou, Y.-Q.; Lu, L.-Q.; Xiao, W.-J. Visible-Light-Induced Organic Photochemical Reactions Through

- Energy-Transfer Pathways. *Angew. Chem. Int. Ed.* **2019**, *58*, 1586–1604.
10. Bauer, A.; Westkämper, F.; Grimme, S.; Bach, T. Catalytic Enantioselective Reactions Driven by Photoinduced Electron Transfer. *Nature* **2005**, *436*, 1139–1140.
11. Nicewicz, D. A.; MacMillan, D. W. C. Merging Photoredox Catalysis with Organocatalysis: The Direct Asymmetric Alkylation of Aldehydes. *Science* **2008**, *322*, 77–80.
12. Brimioulle, R.; Lenhart, D.; Maturi, M. M.; Bach, T. Enantioselective Catalysis of Photochemical Reactions. *Angew. Chem. Int. Ed.* **2015**, *54*, 3872–3890.
13. Meggers, E. Asymmetric Catalysis Activated by Visible Light. *Chem. Commun.* **2015**, *51*, 3290–3301.
14. Wang, C.; Lu, Z. Catalytic Enantioselective Organic Transformations via Visible Light Photocatalysis. *Org. Chem. Front.* **2015**, *2*, 179–190.
15. Silvil, M.; Melchiorre, P. Enhancing the Potential of Enantioselective Organocatalysis with Light. *Nature* **2018**, *554*, 41–49.
16. Skubi, K. L.; Blum, T. R.; Yoon, T. P. Dual Catalysis Strategies in Photochemical Synthesis. *Chem. Rev.* **2016**, *116*, 10035–10074.
17. Zhang, H.-H.; Chen, H.; Zhu, C.; Yu, S. A Review of Enantioselective Dual Transition Metal/Photoredox Catalysis. *Sci. China Chem.* **2020**, *63*, 637–647.
18. Proctor, R. S. J.; Colgan, A. C.; Phipps, R. J. Exploiting Attractive Non-Covalent Interactions for the Enantioselective Catalysis of Reactions Involving Radical Intermediates. *Nat. Chem.* **2020**, *12*, 990–1004.
19. Lipp, A.; Badir, S. O.; Molander, G. A. Stereinduction in Metallaphotoredox Catalysis. *Angew. Chem. Int. Ed.* **2021**, *60*, 1714–1726.
20. Schmermund, L.; Jurkas, V.; Özgen, F. F.; Barone, G. D.; Büchenschütz, H. C.; Winkler, C. K.; Schmidt, S.; Kourist, R.; Kroutil, W. Photo-Biocatalysis: Biotransformations in the Presence of Light. *ACS Catal.* **2019**, *9*, 4115–4144.
21. Mukherjee, S.; Yang, J. W.; Hoffmann, S.; List, B. Asymmetric Enamine Catalysis. *Chem. Rev.* **2007**, *107*, 5471–5569.
22. Capacci, A. G.; Malinowski, J. T.; McAlpine, N. J.; Kuhne, J.; MacMillan, D. W. C. Direct, Enantioselective α -Alkylation of Aldehydes Using Simple Olefins. *Nat. Chem.* **2017**, *9*, 1073–1077.
23. Govender, T.; Arvidsson, P. I.; Maguire, G. E. M.; Kruger, H. G.; Naicker, T. Enantioselective Organocatalyzed Transformations of β -Ketoesters. *Chem. Rev.* **2016**, *116*, 9375–9437.
24. Zhu, Y.; Zhang, L.; Luo, S. Asymmetric α -Photoalkylation of β -Ketocarboxyls by Primary Amine Catalysis: Facile Access to Acyclic All-Carbon Quaternary Stereocenters. *J. Am. Chem. Soc.* **2014**, *136*, 14642–14645.
25. Zhang, L.; Fu, N.; Luo, S. Pushing the Limits of Aminocatalysis: Enantioselective Transformations of α -Branched β -Ketocarboxyls and Vinyl Ketones by Chiral Primary Amines. *Acc. Chem. Res.* **2015**, *48*, 986–997.
26. Huang, M.; Zhang, L.; Pan, T.; Luo, S. Deracemization Through Photochemical E/Z Isomerization of Enamines. *Science* **2022**, *375*, 869–874.
27. Erkkilä, A.; Majander, I.; Pihko, P. M. Iminium Catalysis. *Chem. Rev.* **2007**, *107*, 5416–5470.
28. Murphy, J. J.; Bastida, D.; Paria, S.; Fagnoni, M.; Melchiorre, P. Asymmetric Catalytic Formation of Quaternary Carbons by Iminium Ion Trapping of Radicals. *Nature* **2016**, *532*, 218–222.
29. Flanigan, D. M.; Romanov-Michailidis, F.; White, N. A.; Rovis, T. Organocatalytic Reactions Enabled by *N*-Heterocyclic Carbenes. *Chem. Rev.* **2015**, *115*, 9307–9387.
30. DiRocco, D. A.; Rovis, T. Catalytic Asymmetric α -Acylation of Tertiary Amines Mediated by a Dual Catalysis Mode: *N*-Heterocyclic Carbene and Photoredox Catalysis. *J. Am. Chem. Soc.* **2012**, *134*, 8094–8097.
31. Choi, H.; Mathi, G. R.; Hong, S.; Hong, S. Enantioselective Functionalization at the C4 Position of Pyridinium Salts through NHC Catalysis. *Nat. Commun.* **2022**, *13*, 1776.
32. Feng, Z.-J.; Xuan, J.; Xia, X.-D.; Ding, W.; Guo, W.; Chen, J.-R.; Zou, Y.-Q.; Lu, L.-Q.; Xiao, W.-J. Direct Sp^3 C–H Acroleination of *N*-Aryltetrahydroisoquinolines by Merging Photoredox Catalysis with Nucleophilic Catalysis. *Org. Biomol. Chem.* **2014**, *12*, 2037–2040.
33. Wei, G.; Zhang, C.; Bureš, F.; Ye, X.; Tan, C.-H.; Jiang, Z. Enantioselective Aerobic Oxidative C(sp^3)–H Olefination of Amines via Cooperative Photoredox and Asymmetric Catalysis. *ACS Catal.* **2016**, *6*, 3708–3712.
34. Knowles, R. R.; Jacobsen, E. N. Attractive Noncovalent Interactions in Asymmetric Catalysis: Links Between Enzymes and Small Molecule Catalysts. *Proc. Natl. Acad. Sci. U. S. A.* **2010**, *107*, 20678–20685.
35. Alonso, R.; Bach, T. A Chiral Thioxanthone as an Organocatalyst for Enantioselective [2+2] Photocycloaddition Reactions Induced by Visible Light. *Angew. Chem. Int. Ed.* **2014**, *53*, 4368–4371.
36. Hölzl-Hobmeier, A.; Bauer, A.; Silva, A. V.; Huber, S. M.; Bannwarth, C.; Bach, T. Catalytic Deracemization of Chiral Allenes by Sensitized Excitation with Visible Light. *Nature* **2018**, *564*, 240–243.
37. Vallavoju, N.; Selvakumar, S.; Jockusch, S.; Sibi, M. P.; Sivaguru, J. Enantioselective Organo-Photocatalysis Mediated by Atropisomeric Thiourea Derivatives. *Angew. Chem. Int. Ed.* **2014**, *53*, 5604–5608.
38. Dell’Amico, L.; Vega-Peçaloza, A.; Cuadros, S.; Melchiorre, P. Enantioselective Organocatalytic Diels-Alder Trapping of Photochemically Generated Hydroxy-*o*-Quinodimethanes. *Angew. Chem. Int. Ed.* **2016**, *55*, 3313–3317.
39. Skubi, K. L.; Kidd, J. B.; Jung, H.; Guzei, I. A.; Baik, M.-H.; Yoon, T. P. Enantioselective Excited-State Photoreactions Controlled by a Chiral Hydrogen-Bonding Iridium Sensitizer. *J. Am. Chem. Soc.* **2017**, *139*, 17186–17192.
40. Brenninger, C.; Jolliffe, J. D.; Bach, T. Chromophore Activation of α,β -Unsaturated Carbonyl Compounds and its Application to Enantioselective Photochemical Reactions. *Angew. Chem. Int. Ed.* **2018**, *57*, 14338–14349.
41. Zheng, J.; Swords, W. B.; Jung, H.; Skubi, K. L.; Kidd, J. B.; Meyer, G. J.; Baik, M.-H.; Yoon, T. P. Enantioselective Intermolecular Excited-State Photoreactions Using a Chiral Ir Triplet Sensitizer: Separating Association from Energy Transfer in Asymmetric Photocatalysis. *J. Am. Chem. Soc.* **2019**, *141*, 13625–13634.

42. Proctor, R. S. J.; Davis, H. J.; Phipps, R. J. Catalytic Enantioselective Minisci-Type Addition to Heteroarenes. *Science* **2018**, *360*, 419–422.
43. Yin, Y.; Dai, Y.; Jia, H.; Li, J.; Bu, L.; Qiao, B.; Zhao, X.; Jiang, Z. Conjugate Addition–Enantioselective Protonation of *N*-Aryl Glycines to α -Branched 2-Vinylazaarenes via Cooperative Photoredox and Asymmetric Catalysis. *J. Am. Chem. Soc.* **2018**, *140*, 6083–6087.
44. Gu, Z.; Zhang, L.; Li, H.; Cao, S.; Yin, Y.; Zhao, X.; Ban, X.; Jiang, Z. Deracemization Through Sequential Photoredox–Neutral and Chiral Brønsted Acid Catalysis. *Angew. Chem. Int. Ed.* **2022**, *61*, e202211241.
45. Pecho, F.; Sempere, Y.; Gramüller, J.; Hörmann, F. M.; Gschwind, R. M.; Bach, T. Enantioselective [2 + 2] Photocycloaddition via Iminium Ions: Catalysis by a Sensitizing Chiral Brønsted Acid. *J. Am. Chem. Soc.* **2021**, *143*, 9350–9354.
46. Shin, N. Y.; Ryss, J. M.; Zhang, X.; Miller, S. J.; Knowles, R. R. Light-Driven Deracemization Enabled by Excited-State Electron Transfer. *Science* **2019**, *366*, 364–369.
47. Roos, C. B.; Demaerel, J.; Graff, D. E.; Knowles, R. R. Enantioselective Hydroamination of Alkenes with Sulfonamides Enabled by Proton-Coupled Electron Transfer. *J. Am. Chem. Soc.* **2020**, *142*, 5974–5979.
48. Xu, E. Y.; Werth, J.; Roos, C. B.; Bendel-Smith, A. J.; Sigman, M. S.; Knowles, R. R. Noncovalent Stabilization of Radical Intermediates in the Enantioselective Hydroamination of Alkenes with Sulfonamides. *J. Am. Chem. Soc.* **2022**, *144*, 18948–18958.
49. Shi, Q.; Xu, M.; Chang, R.; Ramanathan, D.; Peñin, B.; Funes-Ardoiz, I.; Ye, J. Visible-Light Mediated Catalytic Asymmetric Radical Deuteration at Non-Benzylic Positions. *Nat. Commun.* **2022**, *13*, 4453.
50. Hashimoto, T.; Maruoka, K. Recent Development and Application of Chiral Phase-Transfer Catalysts. *Chem. Rev.* **2007**, *107*, 5656–5682.
51. Wozniak, Ł.; Murphy, J. J.; Melchiorre, P. Photo-Organocatalytic Enantioselective Perfluoroalkylation of β -Ketoesters. *J. Am. Chem. Soc.* **2015**, *137*, 5678–5681.
52. Uraguchi, D.; Kinoshita, N.; Kizu, T.; Ooi, T. Synergistic Catalysis of Ionic Brønsted Acid and Photosensitizer for a Redox Neutral Asymmetric α -Coupling of *N*-Arylamino-methanes with Aldimines. *J. Am. Chem. Soc.* **2015**, *137*, 13768–13771.
53. Das, S.; Zhu, C.; Demirbas, D.; Bill, E.; De, C. K.; List, B. Asymmetric Counteranion-Directed Photoredox Catalysis. *Science* **2023**, *379*, 494–499.
54. Yang, Z.; Liao, Y.; Zhang, Z.; Chen, J.; Zhang, X.; Liao, S. Asymmetric Ion-Pairing Photoredox Catalysis for Stereoselective Cationic Polymerization Under Light Control. *J. Am. Chem. Soc.* **2024**, *146*, 6449–6455.
55. Guo, H.; Herdtweck, E.; Bach, T. Enantioselective Lewis Acid Catalysis in Intramolecular [2+2] Photocycloaddition Reactions of Coumarins. *Angew. Chem. Int. Ed.* **2010**, *49*, 7782–7785.
56. Zhang, W.; Zhang, L.; Luo, S. Catalytic Asymmetric Visible-Light de Mayo Reaction by $ZrCl_4$ -Chiral Phosphoric Acid Complex. *J. Am. Chem. Soc.* **2023**, *145*, 14227–14232.
57. Onneken, C.; Morack, T.; Soika, J.; Sokolova, O.; Niemeyer, N.; Mück-Lichtenfeld, C.; Daniliuc, C. G.; Neugebauer, J.; Gilmour, R. Light-Enabled Deracemization of Cyclopropanes by Al-salen Photocatalysis. *Nature* **2023**, *621*, 753–759.
58. Wen, L.; Ding, J.; Duan, L.; Wang, S.; An, Q.; Wang, H.; Zuo, Z. Multiplicative Enhancement of Stereoenrichment by a Aingle Catalyst for Deracemization of Alcohols. *Science* **2023**, *382*, 458–464.
59. Poplata, S.; Tröster, A.; Zou, Y.-Q.; Bach, T. Recent Advances in the Synthesis of Cyclobutanes by Olefin [2 + 2] Photocycloaddition Reactions. *Chem. Rev.* **2016**, *116*, 9748–9815.
60. Blum, T. R.; Miller, Z. D.; Bates, D. M.; Guzei, I. A.; Yoon, T. P. Enantioselective Photochemistry Through Lewis Acid-Catalyzed Triplet Energy Transfer. *Science* **2016**, *354*, 1391–1395.
61. Huang, X.; Meggers, E. Asymmetric Photocatalysis with Bis-cyclometalated Rhodium Complexes. *Acc. Chem. Res.* **2019**, *52*, 833–847.
62. Huang, X.; Quinn, T. R.; Harms, K.; Webster, R. D.; Zhang, L.; Wiest, O.; Meggers, E. Direct Visible-Light-Excited Asymmetric Lewis Acid Catalysis of Intermolecular [2+2] Photocycloadditions. *J. Am. Chem. Soc.* **2017**, *139*, 9120–9123.
63. Du, J.; Skubi, K. L.; Schultz, D. M.; Yoon, T. P. A Dual-Catalysis Approach to Enantioselective [2+2] Photocycloadditions Using Visible Light. *Science* **2014**, *344*, 392–396.
64. Huo, H.; Harms, K.; Meggers, E. Catalytic, Enantioselective Addition of Alkyl Radicals to Alkenes via Visible-Light-Activated Photoredox Catalysis with a Chiral Rhodium Complex. *J. Am. Chem. Soc.* **2016**, *138*, 6936–6939.
65. Zhang, K.; Lu, L.-Q.; Jia, Y.; Wang, Y.; Lu, F.-D.; Pan, F.; Xiao, W.-J. Exploration of a Chiral Cobalt Catalyst for Visible-Light-Induced Enantioselective Radical Conjugate Addition. *Angew. Chem. Int. Ed.* **2019**, *58*, 13375–13379.
66. Huo, H.; Shen, X.; Wang, C.; Zhang, L.; Röse, P.; Chen, L.-A.; Harms, K.; Marsch, M.; Hilt, G.; Meggers, E. Asymmetric Photoredox Transition-Metal Catalysis Activated by Visible Light. *Nature* **2014**, *515*, 100–103.
67. Ding, W.; Lu, L.-Q.; Zhou, Q.-Q.; Wei, Y.; Chen, J.-R.; Xiao, W.-J. Bifunctional Photocatalysts for Enantioselective Aerobic Oxidation of β -Ketoesters. *J. Am. Chem. Soc.* **2017**, *139*, 63–66.
68. Li, Y.; Zhou, K.; Wen, Z.; Cao, S.; Shen, X.; Lei, M.; Gong, L. Copper(II)-Catalyzed Asymmetric Photoredox Reactions: Enantioselective Alkylation of Imines Driven by Visible Light. *J. Am. Chem. Soc.* **2018**, *140*, 15850–15858.
69. Li, F.; Tian, D.; Fan, Y.; Lee, R.; Lu, G.; Yin, Y.; Qiao, B.; Zhao, X.; Xiao, Z.; Jiang, Z. Chiral Acid-Catalysed Enantioselective C–H Functionalization of Toluene and Its Derivatives Driven by Visible Light. *Nat. Commun.* **2019**, *10*, 1774.
70. Hou, L.; Zhou, Y.; Yu, H.; Zhan, T.; Cao, W.; Feng, X. Enantioselective Radical Addition to Ketones Through Lewis Acid-Enabled Photoredox Catalysis. *J. Am. Chem. Soc.* **2022**, *144*, 22140–22149.
71. Twilton, J.; Le, C.; Zhang, P.; Shaw, M. H.; Evans, R. W.; MacMillan, D. W. C. The Merger of Transition Metal and Photocatalysis. *Nat. Rev. Chem.* **2017**, *1*, 0052.

72. Fu, G. C. Transition-Metal Catalysis of Nucleophilic Substitution Reactions: A Radical Alternative to S_N1 and S_N2 Processes. *ACS Cent. Sci.* **2017**, *3*, 692–700.
73. Lucas, E. L.; Jarvo, E. R. Stereospecific and Stereoconvergent Cross-Couplings Between Alkyl Electrophiles. *Nat. Rev. Chem.* **2017**, *1*, 0065.
74. Tellis, J. C.; Primer, D. N.; Molander, G. A. Single-Electron Transmetalation in Organoboron Cross-Coupling by Photoredox/Nickel Dual Catalysis. *Science* **2014**, *345*, 433–436.
75. Zuo, Z.; Ahneman, D. T.; Chu, L.; Terrett, J. A.; Doyle, A. G.; MacMillan, D. W. C. Merging Photoredox with Nickel Catalysis: Coupling of α -Carboxyl Sp³-Carbons with Aryl Halides. *Science* **2014**, *345*, 437–440.
76. Zuo, Z.; Cong, H.; Li, W.; Choi, J.; Fu, G. C.; MacMillan, D. W. C. Enantioselective Decarboxylative Arylation of α -Amino Acids via the Merger of Photoredox and Nickel Catalysis. *J. Am. Chem. Soc.* **2016**, *138*, 1832–1835.
77. Stache, E. E.; Rovis, T.; Doyle, A. G. Dual Nickel- and Photoredox-Catalyzed Enantioselective Desymmetrization of Cyclic Meso-Anhydrides. *Angew. Chem. Int. Ed.* **2017**, *56*, 3679–3683.
78. Gandolfo, E.; Tang, X.; Roy, S. R.; Melchiorre, P. Photochemical Asymmetric Nickel-Catalyzed Acyl Cross-Coupling. *Angew. Chem. Int. Ed.* **2019**, *58*, 16854–16858.
79. Cheng, X.; Lu, H.; Lu, Z. Enantioselective Benzylic C–H Arylation via Photoredox and Nickel Dual Catalysis. *Nat. Commun.* **2019**, *10*, 3549.
80. Guan, H.; Zhang, Q.; Walsh, P. J.; Mao, J. Nickel/Photoredox-Catalyzed Asymmetric Reductive Cross-Coupling of Racemic α -Chloro Esters with Aryl Iodides. *Angew. Chem. Int. Ed.* **2020**, *59*, 5172–5177.
81. Zheng, P.; Zhou, P.; Wang, D.; Xu, W.; Wang, H.; Xu, T. Dual Ni/Photoredox-Catalyzed Asymmetric Cross-Coupling to Access Chiral Benzylic Boronic Esters. *Nat. Commun.* **2021**, *12*, 1646.
82. Zhou, P.; Li, X.; Wang, D.; Xu, T. Dual Nickel- and Photoredox-Catalyzed Reductive Cross-Coupling to Access Chiral Trifluoromethylated Alkanes. *Org. Lett.* **2021**, *23*, 4683–4687.
83. Wang, H.; Zheng, P.; Wu, X.; Li, Y.; Xu, T. Modular and Facile Access to Chiral α -Aryl Phosphates via Dual Nickel- and Photoredox-Catalyzed Reductive Cross-Coupling. *J. Am. Chem. Soc.* **2022**, *144*, 3989–3997.
84. Xu, S.; Ping, Y.; Li, W.; Guo, H.; Su, Y.; Li, Z.; Wang, M.; Kong, W. Enantioselective C(sp³)-H Functionalization of Oxacycles via Photo-HAT/Nickel Dual Catalysis. *J. Am. Chem. Soc.* **2023**, *145*, 5231–5241.
85. Fan, P.; Lan, Y.; Zhang, C.; Wang, C. Nickel/Photo-Catalyzed Asymmetric Acyl-Carbamoylation of Alkenes. *J. Am. Chem. Soc.* **2020**, *142*, 2180–2186.
86. Hossain, A.; Bhattacharyya, A.; Reiser, O. Copper's Rapid Ascent in Visible-Light Photoredox Catalysis. *Science* **2019**, *364*, eaav9713.
87. Kainz, Q. M.; Matier, C. D.; Bartoszewicz, A.; Zultanski, S. L.; Peters, J. C.; Fu, G. C. Asymmetric Copper-Catalyzed C–N Cross-Couplings Induced by Visible Light. *Science* **2016**, *351*, 681–684.
88. Lee, H.; Ahn, J. M.; Oyala, P. H.; Citek, C.; Yin, H.; Fu, G. C.; Peters, J. C. Investigation of the C–N Bond-Forming Step in a Photoinduced, Copper-Catalyzed Enantioconvergent *N*-Alkylation: Characterization and Application of a Stabilized Organic Radical as a Mechanistic Probe. *J. Am. Chem. Soc.* **2022**, *144*, 4114–4123.
89. Wang, D.; Zhu, N.; Chen, P.; Lin, Z.; Liu, G. Enantioselective Decarboxylative Cyanation Employing Cooperative Photoredox Catalysis and Copper Catalysis. *J. Am. Chem. Soc.* **2017**, *139*, 15632–15635.
90. Zhang, W.; Wang, F.; McCann, S. D.; Wang, D.; Chen, P.; Stahl, S. S.; Liu, G. Enantioselective Cyanation of Benzylic C–H Bonds via Copper-Catalyzed Radical Relay. *Science* **2016**, *353*, 1014–1018.
91. Nakafuku, K. M.; Zhang, Z.; Wappes, E. A.; Stateman, L. M.; Chen, A. D.; Nagib, D. A. Enantioselective Radical C–H Amination for the Synthesis of β -Amino Alcohols. *Nat. Chem.* **2020**, *12*, 697–704.
92. Lu, F.-D.; Liu, D.; Zhu, L.; Lu, L.-Q.; Yang, Q.; Zhou, Q.-Q.; Wei, Y.; Lan, Y.; Xiao, W.-J. Asymmetric Propargylic Radical Cyanation Enabled by Dual Organophotoredox and Copper Catalysis. *J. Am. Chem. Soc.* **2019**, *141*, 6167–6172.
93. Lu, F.-D.; Lu, L.-Q.; He, G.-F.; Bai, J.-C.; Xiao, W.-J. Enantioselective Radical Carbocyanation of 1,3-Dienes via Photocatalytic Generation of Allylcopper Complexes. *J. Am. Chem. Soc.* **2021**, *143*, 4168–4173.
94. Xia, H.-D.; Li, Z.-L.; Gu, Q.-S.; Dong, X.-Y.; Fang, J.-H.; Du, X.-Y.; Wang, L.-L.; Liu, X.-Y. Photoinduced Copper-Catalyzed Asymmetric Decarboxylative Alkynylation with Terminal Alkynes. *Angew. Chem. Int. Ed.* **2020**, *59*, 16926–16932.
95. Zhang, Y.; Sun, Y.; Chen, B.; Xu, M.; Li, C.; Zhang, D.; Zhang, G. Copper-Catalyzed Photoinduced Enantioselective Dual Carbonylfunctionalization of Alkenes. *Org. Lett.* **2020**, *22*, 1490–1494.
96. Jia, Y.; Zhang, Z.; Yu, G.-M.; Jiang, X.; Lu, L.-Q.; Xiao, W.-J. Visible Light Induced Copper-Catalyzed Enantioselective Deaminative Arylation of Amino Acid Derivatives Assisted by Phenol. *Angew. Chem. Int. Ed.* **2023**, *62*, e202312102.
97. Li, C.; Chen, B.; Ma, X.; Mo, X.; Zhang, G. Photo-Promoted Copper-Catalyzed Enantioselective Alkylation of Azoles. *Angew. Chem. Int. Ed.* **2021**, *60*, 2130–2134.
98. Chen, C.; Peters, J. C.; Fu, G. C. Photoinduced Copper-Catalyzed Asymmetric Amidation via Ligand Cooperativity. *Nature* **2021**, *596*, 250–256.
99. Chen, J.; Liang, Y.-J.; Wang, P.-Z.; Li, G.-Q.; Zhang, B.; Qian, H.; Huan, X.-D.; Guan, W.; Xiao, W.-J.; Chen, J.-R. Photoinduced Copper-Catalyzed Asymmetric C–O Cross-Coupling. *J. Am. Chem. Soc.* **2021**, *143*, 13382–13392.
100. Xu, P.; Fan, W.; Chen, P.; Liu, G. Enantioselective Radical Trifluoromethylation of Benzylic C–H Bonds via Cooperative Photoredox and Copper Catalysis. *J. Am. Chem. Soc.* **2022**, *144*, 13468–13474.
101. Qi, R.; Wang, C.; Huo, Y.; Chai, H.; Wang, H.; Ma, Z.; Liu, L.; Wang, R.; Xu, Z. Visible Light Induced Cu-Catalyzed Asymmetric C(sp³)-H Alkylation. *J. Am. Chem. Soc.* **2021**, *143*, 12777–12783.

102. Ueda, Y.; Masuda, Y.; Iwai, T.; Imaeda, K.; Takeuchi, H.; Ueno, K.; Gao, M.; Hasegawa, J.; Sawamura, M. Photoinduced Copper-Catalyzed Asymmetric Acylation of Allylic Phosphates with Acylsilanes. *J. Am. Chem. Soc.* **2022**, *144*, 2218–2224.
103. Salomon, R. G. Homogeneous Metal-Catalysis in Organic Photochemistry. *Tetrahedron* **1983**, *39*, 485–575.
104. Zhang, H.; Huang, C.; Yuan, X.-A.; Yu, S. Photoexcited Chiral Copper Complex-Mediated Alkene E → Z Isomerization Enables Kinetic Resolution. *J. Am. Chem. Soc.* **2022**, *144*, 10958–10967.
105. Gil, A.; Albericio, F.; Álvarez, M. Role of the Nozaki-Hiyama-Takai-Kishi Reaction in the Synthesis of Natural Products. *Chem. Rev.* **2017**, *117*, 8420–8446.
106. Schwarz, J. L.; Schafers, F.; Tlahuext-Aca, A.; Lückemeier, L.; Glorius, F. Diastereoselective Allylation of Aldehydes by Dual Photoredox and Chromium Catalysis. *J. Am. Chem. Soc.* **2018**, *140*, 12705–12709.
107. Schwarz, J. L.; Huang, H.-M.; Paulisch, T. O.; Glorius, F. Dialkylation of 1,3-Dienes by Dual Photoredox and Chromium Catalysis. *ACS Catal.* **2020**, *10*, 1621–1627.
108. Hu, H.; Shi, Z.; Guo, X.; Zhang, F.-H.; Wang, Z. A Radical Approach for Asymmetric α -C–H Addition of *N*-Sulfonyl Benzylamines to Aldehydes. *J. Am. Chem. Soc.* **2024**, *146*, 5316–5323.
109. Li, Y.-L.; Zhang, S.-Q.; Chen, J.; Xia, J.-B. Highly Regio- and Enantioselective Reductive Coupling of Alkynes and Aldehydes via Photoredox Cobalt Dual Catalysis. *J. Am. Chem. Soc.* **2021**, *143*, 7306–7313.
110. Jiang, X.; Jiang, H.; Yang, Q.; Cheng, Y.; Lu, L.-Q.; Tunge, J. A.; Xiao, W.-J. Photoassisted Cobalt-Catalyzed Asymmetric Reductive Grignard-Type Addition of Aryl Iodides. *J. Am. Chem. Soc.* **2022**, *144*, 8347–8354.
111. Jiang, H.; He, X.-K.; Jiang, X.; Zhao, W.; Lu, L.-Q.; Cheng, Y.; Xiao, W.-J. Photoinduced Cobalt-Catalyzed Desymmetrization of Dialdehydes to Access Axial Chirality. *J. Am. Chem. Soc.* **2023**, *145*, 6944–6952.
112. Jiang, X.; Xiong, W.; Deng, S.; Lu, F.-D.; Jia, Y.; Yang, Q.; Xue, L.-Y.; Qi, X.; Tunge, J. A.; Lu, L.-Q.; Xiao, W.-J. Construction of Axial Chirality via Asymmetric Radical Trapping by Cobalt Under Visible Light. *Nat. Catal.* **2022**, *5*, 788–797.
113. Xiong, W.; Jiang, X.; Wang, W.-C.; Cheng, Y.; Lu, L.-Q.; Gao, K.; Xiao, W.-J. Dynamic Kinetic Reductive Conjugate Addition for Construction of Axial Chirality Enabled by Synergistic Photoredox/Cobalt Catalysis. *J. Am. Chem. Soc.* **2023**, *145*, 7983–7991.
114. Teng, M.-Y.; Liu, D.-Y.; Mao, S.-Y.; Wu, X.; Chen, J.-H.; Zhong, M.-Y.; Huang, F.-R.; Yao, Q.-J.; Shi, B.-F. Asymmetric Dearomatization of Indoles Through Cobalt-Catalyzed Enantioselective C–H Functionalization Enabled by Photocatalysis. *Angew. Chem. Int. Ed.* **2024**, *63*, e202407640.
115. Zhang, M.-M.; Wang, Y.-N.; Lu, L.-Q.; Xiao, W.-J. Light Up the Transition Metal-Catalyzed Single-Electron Allylation. *Trends Chem.* **2020**, *2*, 764–775.
116. Lang, S. B.; O’Nele, K. M.; Tunge, J. A. Decarboxylative Allylation of Amino Alkanoic Acids and Esters via Dual Catalysis. *J. Am. Chem. Soc.* **2014**, *136*, 13606–13609.
117. Xuan, J.; Zeng, T.-T.; Feng, Z.-J.; Deng, Q.-H.; Chen, J.-R.; Lu, L.-Q.; Xiao, W.-J.; Alper, H. Redox-Neutral α -Allylation of Amines by Combining Palladium Catalysis and Visible-Light Photoredox Catalysis. *Angew. Chem. Int. Ed.* **2015**, *54*, 1625–1628.
118. Lang, S. B.; O’Nele, K. M.; Douglas, J. T.; Tunge, J. A. Dual Catalytic Decarboxylative Allylations of α -Amino Acids and Their Divergent Mechanisms. *Chem. Eur. J.* **2015**, *21*, 18589–18593.
119. Zhang, H.-H.; Zhao, J.-J.; Yu, S. Enantioselective Allylic Alkylation with 4-Alkyl-1,4-Dihydropyridines Enabled by Photoredox/Palladium Cocatalysis. *J. Am. Chem. Soc.* **2018**, *140*, 16914–16919.
120. Cheung, K. P. S.; Fang, J.; Mukherjee, K.; Mhraryan, A.; Gevorgyan, V. Asymmetric Intermolecular Allylic C–H Amination of Alkenes with Aliphatic Amines. *Science* **2022**, *378*, 1207–1213.
121. Song, C.; Bai, X.; Li, B.; Dang, Y.; Yu, S. Photoexcited Palladium-Catalyzed Deracemization of Allenes. *J. Am. Chem. Soc.* **2024**, *146*, 21137–21146.
122. Allen, A. D.; Tidwell, T. T. Ketenes and Other Cumulenes as Reactive Intermediates. *Chem. Rev.* **2013**, *113*, 7287–7342.
123. Li, M.-M.; Wei, Y.; Liu, J.; Chen, H.-W.; Lu, L.-Q.; Xiao, W.-J. Sequential Visible-Light Photoactivation and Palladium Catalysis Enabling Enantioselective [4+2] Cycloadditions. *J. Am. Chem. Soc.* **2017**, *139*, 14707–14713.
124. Cheng, Q.; Tu, H.-F.; Zheng, C.; Qu, J.-P.; Helmchen, G.; You, S.-L. Iridium-Catalyzed Asymmetric Allylic Substitution Reactions. *Chem. Rev.* **2019**, *119*, 1855–1969.
125. Crisenza, G. E. M.; Faraone, A.; Gandolfo, E.; Mazzarella, D.; Melchiorre, P. Catalytic Asymmetric C–C Cross-Couplings Enabled by Photoexcitation. *Nat. Chem.* **2021**, *13*, 575–580.
126. Rössler, S. L.; Petrone, D. A.; Carreira, E. M. Iridium-Catalyzed Asymmetric Synthesis of Functionally Rich Molecules Enabled by (Phosphoramidite,Olefin) Ligands. *Acc. Chem. Res.* **2019**, *52*, 2657–2672.
127. Yang, P.; Wang, R.-X.; Huang, X.-L.; Cheng, Y.-Z.; You, S.-L. Enantioselective Synthesis of Cyclobutane Derivatives via Cascade Asymmetric Allylic Etherification/[2+2] Photocycloaddition. *J. Am. Chem. Soc.* **2023**, *145*, 21752–21759.
128. Shang, R.; Ilies, L.; Nakamura, E. Iron-Catalyzed C–H Bond Activation. *Chem. Rev.* **2017**, *117*, 9086–9139.
129. Wang, H.-H.; Shao, H.; Huang, G.; Fan, J.; To, W.-P.; Dang, L.; Liu, Y.; Che, C.-M. Chiral Iron Porphyrins Catalyze Enantioselective Intramolecular C(sp³)–H Bond Amination Upon Visible-Light Irradiation. *Angew. Chem. Int. Ed.* **2023**, *62*, e202218577.
130. Zhang, Y.; Tanabe, Y.; Kuriyama, S.; Sakata, K.; Nishibayashi, Y. Interplay of Diruthenium Catalyst in Controlling Enantioselective Propargylic Substitution Reactions with Visible Light-Generated Alkyl Radicals. *Nat. Commun.* **2023**, *14*, 859.